UPTEC F10 047
Examensarbete 20 p
Augusti 2010

Generation of the Bound Entangled Smolin State and Entanglement Witnesses for Low-Dimensional Unitary Invariant States

Emil Nordling

UPPSALA
UNIVERSITET

Teknisk- naturvetenskaplig fakultet
UTH-enheten

Besöksadress:
Ångströmlaboratoriet
Lägerhyddsvägen 1
Hus 4, Plan 0

Postadress:
Box 536
751 21 Uppsala

Telefon:
018 – 471 30 03

Telefax:
018 – 471 30 00

Hemsida:
http://www.teknat.uu.se/student

Abstract

Generation of the Bound Entangled Smolin State and Entanglement Witnesses for Low-Dimensional Unitary Invariant States

Emil Nordling

Quantum entanglement is employed as a resource throughout quantum information science. However, before entanglement can be put to intelligent use, the issues of its production and detection must be considered.
This thesis proposes four schemes for producing the bound entangled Smolin state. Three of these schemes produce the Smolin state by means of general quantum gates acting on different initial states - an all-zero state, a GHZ-state and two combined Bell states. The fourth scheme is based on one-qubit operations acting on two-photon states produced by SPDC.
Furthermore, a maximum overlap entanglement witness detecting entanglement in the Smolin state is derived. This witness is measurable in three measurement settings with the maximal noise tolerance p=2/3.
Lastly, simplified entanglement witnesses for the 4-, 6- and 8-qubit unitary invariant states are derived. These witnesses are measurable in three measurement settings with noise tolerances p=0.1802..., p=0.1502... and p=0.0751..., respectively.

Handledare: Doc. Mohamed Bourennane
Ämnesgranskare: Prof. Ulf Danielsson
Examinator: Dr. Tomas Nyberg
ISSN: 1401-5757, UPTEC F10 047

Generation of the Bound Entangled Smolin State and Entanglement Witnesses for Low-Dimensional Unitary Invariant States

Emil Nordling
The Master Programme in Engineering Physics
Applied Physics Branch
Uppsala University

August 22, 2010

Abstract

Quantum entanglement is employed as a resource throughout quantum information science. However, before entanglement can be put to intelligent use, the issues of its production and detection must be considered.

This thesis proposes four schemes for producing the bound entangled Smolin state. Three of these schemes produce the Smolin state by means of general quantum gates acting on different initial states - an all-zero state, a GHZ-state and two combined Bell states. The fourth scheme is based on one-qubit operations acting on two-photon states produced by SPDC.

Furthermore, a maximum overlap entanglement witness detecting entanglement in the Smolin state is derived. This witness is measurable in three measurement settings with the maximal noise tolerance p=2/3.

Lastly, simplified entanglement witnesses for the 4-, 6- and 8-qubit unitary invariant states are derived. These witnesses are measurable in three measurement settings with noise tolerances p=0.1802..., p=0.1502... and p=0.0751..., respectively.

CONTENTS

CHAPTER 1

INTRODUCTION

In the distance I could hear
Words of wisdom whizzing by my ear
- S. S. V.

Entanglement is the "spooky action at a distance"[1] which makes certain composite quantum systems[1] behave as if its components were connected, regardless of the isolation and spatial distance between these components.
The connection in an entangled system is such that observations of one part of the system correlate to observations of some other part, with correlations stronger than classical physics will allow.
Indeed, entanglement follows as a natural consequence of the principles of quantum mechanics, whereas a classical treatment of the subject leads to a number of difficulties and paradoxes[2].

The premise for entanglement is that once two systems have interacted, they should be regarded as one single system. A full description of the constitutent parts by themselves does not necessarily give full knowledge of the behavior of the system as a whole[2].

The correlations of entangled states were first recognized by Schrödinger as a *Verschränkung der Voraussagen*[3], roughly *Entanglement of Predictions*, referring to the intertwined predictions made by quantum theory about the outcomes of measurements on entangled systems.
The non-local properties of entanglement, the "spooky action at a distance", which makes it utterly incompatible with classical physics, led Einstein, Podolsky and Rosen (EPR) to propose the idea that quantum mechanics needed extra, or hidden, variables to explain the non-locality while remaining a local theory[4]. However, should such hidden variables exist, the theory of quantum mechanics would be rendered incomplete. Later, in a seminal paper[5], Bell presented an upper limit of the strength of the correlations of local hidden

[1] E.g. two electrons, two photons or two atoms.

variable theories such as the one laid out by EPR. It turned out that quantum mechanical experiments with entangled particles, notably those of Aspect et al.[6], violated this limit, thus refuting EPR and implying that quantum mechanics is indeed a complete non-local theory *sans* hidden variables.

The field of quantum computation emerged in the early 1980's with the realization that certain calculations could be elegantly performed using the features of quantum mechanics. The simulation of quantum systems is a natural example of such a computation, since quantum systems obviously would simulate themselves best[7]. However, quantum computation extends beyond problems in the quantum realm, providing faster, albeit probabilistic, solutions to classically hard problems[8]. The ultimate goal, however distant, is a general purpose quantum computer, which would be able to solve diverse problems without the need for redesigning the computer hardware for each new type of computation[9]. To specific quantum algorithms, as well as to general quantum computers, entanglement provides parallelism impossible to reach by classical means[8] and a means to transport arbitrary quantum states by teleportation[10].

For quantum computation, entanglement is a resource as real and useful as electric current and electric voltage are for classical systems, and like these quantities, entanglement can easily be disturbed by extraneous interference. Entanglement that has been degraded can be improved by a process known as *distillation*. The process involves gathering several degraded, but still slightly entangled states and by means of local quantum operations and classical communication producing one or several highly entangled states[12]. The discovery of *bound entangled entangled states*, states that contain entanglement but cannot be distilled, provide a means to examine the phenomenon of distillability in its seams. The *Smolin bound entangled four-partite state*[13] takes a special place among other bound entangled states due to its symmetric construction and its *unlockable* entanglement. The unlockability means that a maximally entangled state can be produced by simply bringing together two of the four subsystems. Discovered in 2000, the Smolin state has since found its place in quantum computation by its application in quantum secret sharing[14] and remote information concentration[15].

An alternative approach to avoid the effects of interference is to choose to operate with entangled states that are not susceptible to certain types of noise[11]. One family of such states, the n-lateral unitary invariant singlet states, are unaffected by the quantum channel along which they are propagated, as long as it untarily transforms each qubit of the state in the same manner. In e.g. a photonic system this means that the common reference direction for the polarization analyzers can be chosen freely, regardless of the orientation of the photon source. Detection and measurement of entanglement content of the 4-lateral unitary invariant state are found in [16].

This report will describe four approaches to producing the Smolin state, along with the machinery needed to examine its entanglement content and analyze its symmetry properties. The report finishes with a chapter presenting simplified entanglement witnesses for the 4-, 6- and 8-qubit unitary invariant singlet states.

CHAPTER 2

THEORY

If it's all right with Dirac, it's all right with me.
- E. F.

Below, the basic elements of the Dirac formalism for quantum mechanics are recapitulated, along with the building blocks for quantum gate networks and photonic systems.

2.1 Hilbert spaces, kets and bras

The *state space* of a quantum mechanical system S is a complex Hilbert space $\mathcal{H}_S$ whose elements $|\psi_i\rangle^S$ are called *kets* [17]. A particular state of S, ψ_S, can be represented by a one-dimensional subspace of $\mathcal{H}_S$, for instance $c|\psi_S\rangle^S$, $c \in \mathbb{C} \setminus 0$. Each ket $|\psi_i\rangle^S$ has one unique dual *bra* ${}^S\langle\psi_i|$ in the dual space $\mathcal{H}_S^*$. The bra corresponding to a ket $|\psi\rangle$ is given by the isomorphism ϕ, $\langle\psi| = \phi(|\psi\rangle)$. ϕ is chosen so that

$$\phi(c|\psi\rangle) = c^*\langle\psi|, \quad c \in \mathbb{C} \tag{2.1.1}$$

$$\phi(|\psi_1\rangle + |\psi_2\rangle) = \phi(|\psi_1\rangle) + \phi(|\psi_2\rangle) = \langle\psi_1| + \langle\psi_2| \tag{2.1.2}$$

2.1.1 Inner product

The inner product of $|\psi_1\rangle$ and $|\psi_2\rangle$ is defined [18]

$$\langle|\psi_1\rangle, |\psi_2\rangle\rangle = \phi(|\psi_1\rangle)|\psi_2\rangle = \langle\psi_1||\psi_2\rangle \equiv \langle\psi_1|\psi_2\rangle \in \mathbb{C}, \tag{2.1.3}$$

which has the following properties

$$\begin{aligned} &\text{Conjugate symmetry:} \\ \langle\psi_1|\psi_2\rangle &= \langle\psi_2|\psi_1\rangle^* && (2.1.4) \\ &\text{Sesquilinearity:} \\ (2.1.1) \Rightarrow \langle a|\psi_1\rangle, b|\psi_2\rangle\rangle &= a^* b\langle\psi_1|\psi_2\rangle && (2.1.5) \\ (2.1.2) \Rightarrow \langle|\psi_1\rangle + |\psi_2\rangle, |\psi_3\rangle + |\psi_4\rangle\rangle &= \langle\psi_1|\psi_3\rangle + \langle\psi_1|\psi_4\rangle \\ &\quad +\langle\psi_2|\psi_3\rangle + \langle\psi_2|\psi_4\rangle. && (2.1.6) \end{aligned}$$

Iff $\langle\psi_1|\psi_2\rangle = 0$, $|\psi_1\rangle$ and $|\psi_2\rangle$ are said to be orthogonal. The isomorphism ϕ guarantees non-degeneracy of the inner product.
For the symmetric product, (2.1.4) leads to $\langle\psi|\psi\rangle \in \mathbb{R}$. Furthermore, non-negativity is postulated

$$\begin{aligned} \langle\psi|\psi\rangle &\geq 0 && (2.1.7) \\ \Rightarrow \langle\psi|\psi\rangle &= 0 \,\text{iff}\, |\psi\rangle = |0\rangle. && (2.1.8) \end{aligned}$$

2.1.2 Norm

The norm of $|\psi\rangle$ is $\||\psi\rangle\| = \sqrt{\langle\psi|\psi\rangle}$. Positive homogeneity, subadditivity and positive definiteness of the norm are guaranteed by its construction.

Provided that a ket $|\psi\rangle$ is not a null ket, it can be normalized

$$|\hat{\psi}\rangle = \frac{1}{\sqrt{\langle\psi|\psi\rangle}}|\psi\rangle. \tag{2.1.9}$$

Since both $|\hat{\psi}\rangle$ and $|\psi\rangle$ both refer to the same physical state, we might as well require that all kets belonging to physical states shall be normalized.

2.1.3 Outer product

The outer product of $|\psi_1\rangle$ and $|\psi_2\rangle$ is defined $|\psi_1\rangle\langle\psi_2|$. Due to its associativity one very useful combination of products is

$$\left(|\psi_1\rangle\langle\psi_2|\right)|\psi_3\rangle = |\psi_1\rangle\left(\langle\psi_2|\psi_3\rangle\right) \tag{2.1.10}$$

2.1.4 Tensorial product

The tensorial product of $|\psi_1\rangle^A$ and $|\psi_2\rangle^B$, belonging to Hilbert spaces $\mathcal{H}_A$ and $\mathcal{H}_B$ respectively, is

$$|\psi_3\rangle^C = |\psi_1\rangle^A \otimes |\psi_2\rangle^B, \tag{2.1.11}$$

where $|\psi_3\rangle^C$ belongs to the composite space $\mathcal{H}_C = \mathcal{H}_A \otimes \mathcal{H}_B$. Also,

$$\bigotimes_{n=1}^{N} |\psi_n\rangle \equiv \underbrace{|\psi_1\rangle \otimes |\psi_2\rangle \otimes \cdots \otimes |\psi_n\rangle}_{N factors} \equiv |\psi_1\psi_2 \ldots \psi_n\rangle \tag{2.1.12}$$

and

$$|\psi\rangle^{\otimes N} \equiv \bigotimes_{n=1}^{N} |\psi\rangle. \tag{2.1.13}$$

Any other product-like combinations, e.g.

$${}^{A}\langle\psi_1|\psi_2\rangle^{B}, \quad |\psi_1\rangle^{A} \in \mathcal{H}_A, \quad |\psi_2\rangle^{B} \in \mathcal{H}_B, \quad \mathcal{H}_A \neq \mathcal{H}_B, \tag{2.1.14}$$

are simply non-sensical and consequently not allowed.

2.1.5 Matrix representation

For a finite-dimensional Hilbert space $\mathcal{H}$ of dimension $\dim(\mathcal{H}) = d$ we can define an orthonormal basis as $\{|\psi_i\rangle\}_{i=1}^{d}$ where $\langle\psi_i|\psi_j\rangle = \delta_{ij}$. Now an arbitrary vector can be represented as[17]

$$|\psi\rangle = \sum_{i=1}^{d} a_i|\psi_i\rangle,\ a_i \in \mathbb{C}$$

where $\sum_{i=1}^{d} a_i^* a_i = 1$ implies that $|\psi\rangle$ is normalized to unity.
The coefficients a_i are

$$a_i = \langle\psi_i|\psi\rangle. \tag{2.1.15}$$

Given the orthonormal basis above, one matrix representation of a ket is

$$|\psi\rangle \doteq \begin{pmatrix} a_1 \\ a_2 \\ \vdots \\ a_d \end{pmatrix}, \tag{2.1.16}$$

The isomorphism between $\mathcal{H}$ and $\mathcal{H}^*$ is represented by a complex conjugation followed by transposition, giving the dual vector of $|\psi\rangle$ as

$$\langle\psi| \doteq \begin{pmatrix} a_1* \\ a_2* \\ \vdots \\ a_d* \end{pmatrix}^{T} = \begin{pmatrix} a_1^* & a_2^* & \dots & a_d^* \end{pmatrix}. \tag{2.1.17}$$

Using the matrix representations of bras and kets the usual theorems of matrix algebra are valid, giving the inner product

$$\begin{aligned} \langle\phi|\psi\rangle \doteq \begin{pmatrix} a_1^* & a_2^* & \dots & a_d^* \end{pmatrix} \begin{pmatrix} b_1 \\ b_2 \\ \vdots \\ b_d \end{pmatrix} &= \sum_{i=1}^{d} a_i^* b_i, \\ |\phi\rangle &= \sum_{i=1}^{d} a_i|\phi_i\rangle,\ |\psi\rangle = \sum_{i=1}^{d} b_i|\psi_i\rangle,\ a_i, b_i \in \mathbb{C}, \end{aligned} \tag{2.1.18}$$

the outer product

$$|\phi\rangle\langle\psi| \doteq \begin{pmatrix} a_1 \\ a_2 \\ \vdots \\ a_d \end{pmatrix} \begin{pmatrix} b_1^* & b_2^* & \dots & b_d^* \end{pmatrix} = \begin{pmatrix} a_1 b_1^* & a_1 b_2^* & \dots & a_1 b_d^* \\ a_2 b_1^* & a_2 b_2^* & \dots & a_2 b_d^* \\ \vdots & \vdots & \ddots & \vdots \\ a_d b_1^* & a_d b_2^* & \dots & a_d b_d^* \end{pmatrix}, \tag{2.1.19}$$

and the tensor product as the Kronecker product

$$|\phi\rangle^A \otimes |\psi\rangle^B \doteq \begin{pmatrix} a_1 \begin{pmatrix} b_1 \\ b_2 \\ \vdots \\ b_e \end{pmatrix} \\ a_2 \begin{pmatrix} b_1 \\ b_2 \\ \vdots \\ b_e \end{pmatrix} \\ \vdots \\ a_d \begin{pmatrix} b_1 \\ b_2 \\ \vdots \\ b_e \end{pmatrix} \end{pmatrix} = \begin{pmatrix} a_1 b_1 \\ a_1 b_2 \\ \vdots \\ a_1 b_e \\ a_2 b_1 \\ a_2 b_2 \\ \vdots \\ a_2 b_e \\ \vdots \\ a_d b_1 \\ a_d b_2 \\ \vdots \\ a_d b_e \end{pmatrix} \tag{2.1.20}$$

$$|\phi\rangle^A = \sum_{i=1}^{d} a_i |\phi_i\rangle^A \in \mathcal{H}_A \text{ and } |\psi\rangle^B = \sum_{i=1}^{e} b_i |\psi_i\rangle^B \in \mathcal{H}_B,\ e = \dim(\mathcal{H}_B).$$

Bases for composite Hilbert spaces are constructed

$$\{|\psi_{ij}\rangle^C\}_{i=1\dots d,\, j=1\dots e},\ |\psi_{ij}\rangle^C = |\phi_i\rangle^A \otimes |\psi_j\rangle^B, \tag{2.1.21}$$

for which the matrix representations are produced in exactly the same manner as above.

2.2 Linear operators

The Dirac formalism allows us to construct linear operators on the Hilbert-space as follows,

$$\Theta = \sum_{i,j=1..d} c_{ij} |\psi_i\rangle\langle\psi_j|,\ c_{ij} \in \mathbb{C}, \tag{2.2.1}$$

where $\{|\psi_i\rangle\}_{i=1}^d$ is an orthonormal basis as those above. Using (2.1.19), the matrix representation of Θ is

$$\Theta \doteq (c_{ij}) \tag{2.2.2}$$

2.2.1 Trace

The trace of a linear operator is defined

$$\mathrm{Tr}(\Theta) = \sum_i \langle\psi_i|\Theta|\psi_i\rangle,$$

where the $|\psi_i\rangle$ belong to an orthonormal basis as above.

2.2.2 Transposition

The transposition Θ^T of a linear operator Θ is simply the operator expansion

$$\Theta = \sum_{i,j=1..d} c_{ij}|\psi_i\rangle\langle\psi_j|,\ c_{ij} \in \mathbb{C}, \tag{2.2.3}$$

with kets and bras reversed

$$\Theta^T = \sum_{i,j=1..d} c_{ij}|\psi_j\rangle\langle\psi_i|,\ c_{ij} \in \mathbb{C}, \tag{2.2.4}$$

In matrix representation this resolves to the normal matrix transpose.

2.2.3 Eigenvalues

The eigenvalue equation in the Dirac formalism is

$$\Theta|\psi\rangle = \theta|\psi\rangle, \quad \theta \in \mathbb{C}, \tag{2.2.5}$$

in analogy with other notational paradigms.

2.2.4 Hermitian adjoint

The Hermitian adjoint of an linear operator is denoted by the dagger † and is a complex conjugation followed by transposition

$$\Theta^\dagger = (\Theta^*)^T \doteq (c_{ij}^*)^T. \tag{2.2.6}$$

It follows that while Θ operates on kets, $\Theta^\dagger$ rather operates on bras

$$\Theta|\psi\rangle = \left(\sum_{i,j=1..d} c_{ij}|\psi_i\rangle\langle\psi_j|\right)|\psi\rangle = \sum_{i,j=1..d} c_{ij}\langle\psi_j|\psi\rangle|\psi_i\rangle \tag{2.2.7}$$

$$\langle\psi|\Theta^\dagger = \langle\psi|\left(\sum_{i,j=1..d} c_{ij}^*|\psi_j\rangle\langle\psi_i|\right) = \sum_{i,j=1..d} c_{ij}^*\langle\psi|\psi_j\rangle\langle\psi_i| \tag{2.2.8}$$

Obviously the result in (2.2.8) is the corresponding bra of (2.2.7).
An operator for which

$$\Theta = \Theta^\dagger \tag{2.2.9}$$

is called *Hermitian*. By the spectral theorem[19], Hermiticity guarantees that the operator has real eigenvalues and orthogonal eigenvectors spanning the Hilbert space.

2.2.5 Observables

An *observable* is a Hermitian operator corresponding to a experimentally measureable quantity. An eigenvalue of an observable is the measurement outcome if the system measured upon was in the corresponding eigenstate.

2.2.6 The density operator

The density operator ρ describes an ensemble of states $|\psi_i\rangle$ along with their probabilistic mixture, given by the coefficients p_i.

$$\rho = \sum_i p_i |\psi_i\rangle\langle\psi_i|, \quad p_i \in \mathbb{R}_+ \quad \text{and} \quad \sum_i p_i = 1,$$

where the $|\psi_i\rangle$ are normalized to unity. This gives ρ the following properties:

$$\rho = \rho^\dagger \quad \text{(Hermiticity)} \tag{2.2.10}$$

$$\forall |\psi\rangle : \langle\psi|\rho|\psi\rangle \geq 0 \quad \text{(Positivity)} \tag{2.2.11}$$

$$\mathrm{Tr}(\rho) = 1 \quad \text{(Unit trace).} \tag{2.2.12}$$

The density operator ρ is sometimes called the *state*[1] of the system, since it provides a full description of the ensemble. A *pure* state refers to the case where only one single state $|\psi_1\rangle$ is present in the ensemble, whereas a *mixed* state ρ contains multiple terms.

2.2.7 Expectation value

The quantity

$$\langle\Theta\rangle = \langle\psi|\Theta|\psi\rangle \tag{2.2.13}$$

corresponds to the expectation value of repeated measurement of observable Θ on the state vector $|\psi\rangle$.
The expectation value of a observable acting on a density operator is given by

$$\langle\Theta\rangle = \mathrm{Tr}(\Theta\rho), \tag{2.2.14}$$

which is easily seen by choosing the orthonormal basis for the trace as the normalized eigenkets of Θ, expanding ρ in this basis and directly calculating (2.2.14).
If the state is an eigenstate of Θ, the mean value is its corresponding eigenvalue.

2.2.8 Spin observables and Pauli matrices

The identity operator along with the spin observables and their corresponding Pauli matrices are:

$$\begin{aligned}
\mathbb{I} \equiv \quad \sigma_0 &= |0\rangle\langle 0| + |1\rangle\langle 1| \doteq \begin{pmatrix} 1 & 0 \\ 0 & 1 \end{pmatrix} \\
\sigma_x \equiv \quad \sigma_1 &= |1\rangle\langle 0| + |0\rangle\langle 1| \doteq \begin{pmatrix} 0 & 1 \\ 1 & 0 \end{pmatrix} \\
\sigma_y \equiv \quad \sigma_2 &= i|1\rangle\langle 0| - i|0\rangle\langle 1| \doteq \begin{pmatrix} 0 & -i \\ i & 0 \end{pmatrix} \\
\sigma_z \equiv \quad \sigma_3 &= |0\rangle\langle 0| - |1\rangle\langle 1| \doteq \begin{pmatrix} 1 & 0 \\ 0 & -1 \end{pmatrix}.
\end{aligned} \tag{2.2.15}$$

σ_0 represents a "null" measurement, retrieving no information about the state of the system. σ_1, σ_2 and σ_3 serve as observables for the spin components of a spin-$\frac{1}{2}$ particle measured

[1] This convention will be used throughout this report, since the reader is not too likely to confuse ensemble states with state *kets* or state *bras*.

along the x-, y- and z-axis respectively. Here, the σ_i are normalized to give ± 1 rather than the usual $\pm\hbar/2$ when acting on their eigenstates.
The σ_i have the properties

$$\sigma_i = \sigma_i^\dagger \qquad \text{(Hermiticity)} \tag{2.2.16}$$

$$\sigma_i^\dagger \sigma_i = \mathbb{I} \qquad \text{(Unitarity)} \tag{2.2.17}$$

$$\sigma_i \sigma_j = \delta_{ij}\mathbb{I} + i\epsilon_{ijk}\sigma_k \qquad \text{(Product property)} \tag{2.2.18}$$

$$\mathrm{Tr}(\sigma_i) = 2\delta_{0i} \qquad \text{(Trace: two or zero)} \tag{2.2.19}$$

$$\mathrm{Tr}(\sigma_i^\dagger \sigma_j) = 2\delta_{ij} \qquad \text{(Mutual orthogonality)} \tag{2.2.20}$$

$$\tag{2.2.21}$$

where in (2.2.18), ϵ_{ijk} is the antisymmetric Levi-Civita symbol which is $+1$ (-1) for $(\mathrm{i}, \mathrm{j}, \mathrm{k})$ that are cyclic (non-cyclic) permutations of $(1, 2, 3)$ and otherwise 0.
The σ_i constitute a basis for all linear operators acting on a two-dimensional Hilbert space; any linear operator on a two-dimensional Hilbert space can be formed as

$$\Theta = \sum_{i=0}^{3} c_i \sigma_i,\ c_i \in \mathbb{C}. \tag{2.2.22}$$

2.2.9 Tensorial product

It is clear that the tensorial product (2.1.11) of kets and bras immediately gives a tensorial product for linear operators on $\mathcal{H}_A$ and $\mathcal{H}_B$ as $\Theta^A \otimes \Theta^B$. Consequently, $\bigotimes_{n=1}^N \Theta_n$ and $\Theta^{\otimes N}$ follow the same conventions as (2.1.12) and (2.1.13).

2.2.10 Local decomposition

The tensorial product of bases of operators on the spaces $\{\mathcal{H}_n\}_{n=1}^N$, $\dim(\mathcal{H}_n) = 2$, provides a basis for operators on the composite space $\mathcal{H}_A = \bigotimes_{n=1}^N \mathcal{H}_n$. Assuming the $\{\sigma_i\}$ is the basis for each subsystem, the elements of the new basis are all the

$$\sigma_{i_1,i_2,\ldots,i_N} = \bigotimes_{n=1}^{N} \sigma_{i_n}, \tag{2.2.23}$$

for which $(i_1, i_2, \ldots, i_N) \in \{0, 1, 2, 3\}^N$.
An arbitrary linear operator on $\mathcal{H}_A$ can now be expressed

$$\begin{aligned} \Theta^A &= \sum_{\forall (i_1,i_2,\ldots,i_N) \in \{0,1,2,3\}^N} c_{i_1,i_2,\ldots,i_N} \sigma_{i_1,i_2,\ldots,i_N} \\ &= \sum_{\forall (i_1,i_2,\ldots,i_N) \in \{0,1,2,3\}^N} c_{i_1,i_2,\ldots,i_N} \bigotimes_{n=1}^{N} \sigma_{i_n}, \\ & c_{i_1,i_2,\ldots,i_N} \in \mathbb{C}, \end{aligned} \tag{2.2.24}$$

where the sum includes all 4^N possible $\sigma_{i_1,i_2,\ldots,i_N}$'s. Since each σ_i acts locally on its subsystem, the expression (2.2.24) is called a *local decomposition* of the operator Θ^A.
For any given linear operator Θ^A on $\mathcal{H}_A$ the coefficients $c_{i_1,i_2,\ldots,i_N}$ are given by

$$c_{i_1,i_2,\ldots,i_N} = \mathrm{Tr}(\Theta^A \sigma_{i_1,i_2,\ldots,i_N}) \tag{2.2.25}$$

A local decomposition of a density operator have to contain σ_0 in order to fulfill (2.2.12) and have $c_{i_1,i_2,\ldots,i_N} \in \mathbb{R}$ to maintain hermiticity (2.2.10), and especially have $c_{0,0,\ldots,0} = 1$ to give (2.2.11).

2.2.11 Partial trace

Let Q^{AB} be an operator on the composite Hilbert space $\mathcal{H}_A \otimes \mathcal{H}_B$, then the partial trace of the part of the system belonging to $\mathcal{H}_A$ is defined by:

$$\mathrm{Tr}_A(Q^{AB}) = \sum_{i=1}^{d_A} {}^A\langle\psi_i|Q^{AB}|\psi_i\rangle^A, \tag{2.2.26}$$

where $\{|\psi_i\rangle^A\}_{i=1}^{d_A}$ is an orthonormal basis in $\mathcal{H}_A$ and d_A the dimension of this space.

2.2.12 Partial transpose

Let Q be an operator on the composite Hilbert space $\mathcal{H}_A \otimes \mathcal{H}_B$, then partial transposition (PT) of $\mathcal{H}_A$ is defined by:

$$Q^{T_A} \equiv (T_A \otimes \mathbb{I}_B)Q, \tag{2.2.27}$$

where T_A is the transposition operator on $\mathcal{H}_A$ while $\mathbb{I}_B$ is the identity operator on $\mathcal{H}_B$. Partial transposition for $\mathcal{H}_B$ is defined analogously.

2.2.13 Local Operations and Classical Communication

Local (quantum) Operations and Classical Communication (LOCC) refers to experiments where the experimenters are restricted to performing local operations on a system and communicating information, e.g. measurement outcomes, among themselves using *only* classical communication[20]. In practice this means that under LOCC, the operators applicable to a composite system A take the form

$$\Theta^A = \bigotimes_i \theta^{a_i}, \tag{2.2.28}$$

where θ^{a_i} are operators on the local subsystems a_i.
LOCC imposes some constraints on what can be done to a quantum system, for instance, one cannot increase the amount of entanglement through LOCC and Bell-measurement, as well as two-qubit quantum gates, are unachievable.

2.2.14 Non-local operations

In contrast to LOCC, non-local operations can be performed on multiple parties under the requirement that the parties involved are brought together. These operations include multi-qubit quantum gates, creation and increase of entanglement and Bell measurement (see section 2.4.2). Non-local operations can be achieved by contructing their operators according to (2.2.1), using *inseparable* states (see section 2.4) as the basis states.

2.3 Ancillary systems

Extra, or *ancillary*, Hilbert spaces may be added to a primary Hilbert space to facilitate certain operations. These operations include the creation of mixtures of states and the selecting of valid subspaces from the primary Hilbert space.

2.3.1 Mixing of States

Let $\{|\phi_i\rangle^A\}_{i=1}^d$ be the states belonging to the primary Hilbert space $\mathcal{H}_A$ to be probabilistically mixed, while the normalized and mutually orthogonal $\{|\psi_i\rangle^B\}_{i=1}^d$ belong to an ancillary Hilbert space $\mathcal{H}_B$, with $d \leq \dim(\mathcal{H}_B)$. Then prepare

$$|\phi\rangle^{AB} = \sum_i c_i |\phi_i\rangle^A |\psi_i\rangle^B, \tag{2.3.1}$$

with $c_i \in \mathbb{C}$ and $\sum_i c_i^2 = 1$. A mixed state is now produced by tracing out the ancillary part.

$$\rho_{mixed} = \mathrm{Tr}_B\left(|\phi\rangle^{AB}\langle\phi|\right) = \sum_i c_i^2 |\phi\rangle_i^A\langle\phi|. \tag{2.3.2}$$

2.3.2 Post-selection

To select a subset of states from a larger set of states produced by an experimental setup, additional criteria may be imposed on the set of states. This *post-selection* can be done using an ancillary system connected to the primary system and projecting the set of composite states on the appropriate ancillary states to yield the subset.
Let $\{\rho_i^A\}_{i=1}^d$ be the set of states belonging to the primary Hilbert space $\mathcal{H}_A$, while the normalized and mutually orthogonal $\{|\psi_i\rangle^B\}_{i=1}^d$ belong to the ancillary Hilbert space $\mathcal{H}_B$. $d \leq \dim(\mathcal{H}_B)$. One possible composite system is given by

$$\rho^{AB} = \sum_i \rho_i^A \otimes |\psi_i\rangle^B\langle\psi_i|.$$

A particular state, e.g. ρ_j^A, $1 \leq j \leq d$, is post-selected by projecting on $|\psi_j\rangle^B$,

$$\rho_{ps} =^B \langle\psi_j|\rho^{AB}|\psi_j\rangle^B = \rho_j^A.$$

Post-selection is often used in multi-detector setups where the experiment might not always produce a particle at each detector. By post-selecting the state with regard to the number of particles at the detectors, one can isolate the circumstance where particles are present at all the detectors.

2.4 Separability and entanglement

A quantum state ρ on $\mathcal{H} = \bigotimes_{i=1}^n \mathcal{H}_i$, $n > 1$, is separable iff it can be written on the form

$$\rho = \sum_j p_j \bigotimes_{i=1}^n \rho_i, \quad p_j \in \mathbb{R}_+ \quad \text{and} \quad \sum_j p_j = 1, \tag{2.4.1}$$

where $\rho_i \in \mathcal{H}_i$.

If no such sum can be found then the state is inseparable, or *entangled*.
If $n = 2$ then the state is called *biseparable* and if $n = 3$ the state is called *triseparable*. In general, if ρ fullfills (2.4.1), n implies n-separability. Obviously,

$$\{\rho : \rho = \sum_j p_j \bigotimes_{i=1}^{n} \rho_i\} \subset \{\rho : \rho = \sum_j p'_j \bigotimes_{i=1}^{n-1} \rho'_i\} \subset ... \subset \{\rho : \rho = \sum_j p''_j \bigotimes_{i=1}^{2} \rho''_i\}. \quad (2.4.2)$$

2.4.1 Bell states and GHZ states

Examples of entangled states are the Bell states, or EPR pairs,

$$\begin{aligned} |\Psi^-\rangle \equiv \quad |\Psi_1\rangle = \quad & \tfrac{1}{\sqrt{2}}(|01\rangle - |10\rangle) \\ |\Psi^+\rangle \equiv \quad |\Psi_2\rangle = \quad & \tfrac{1}{\sqrt{2}}(|01\rangle + |10\rangle) \\ |\Phi^+\rangle \equiv \quad |\Psi_3\rangle = \quad & \tfrac{1}{\sqrt{2}}(|00\rangle + |11\rangle) \\ |\Phi^-\rangle \equiv \quad |\Psi_4\rangle = \quad & \tfrac{1}{\sqrt{2}}(|00\rangle - |11\rangle), \end{aligned} \quad (2.4.3)$$

and the GHZ n-qubit state

$$|GHZn\rangle = \frac{1}{\sqrt{2}}(|0\rangle^{\otimes n} + |1\rangle^{\otimes n}),\ n \geq 3. \quad (2.4.4)$$

From the local decomposition of e.g. $\rho_{\Psi^-} = |\Psi^-\rangle\langle\Psi^-|$,

$$\rho_{\Psi^-} = \frac{1}{4}(\mathbb{I} \otimes \mathbb{I} - \sigma_x \otimes \sigma_x - \sigma_y \otimes \sigma_y - \sigma_z \otimes \sigma_z),$$

it can be seen that it does not factor into an expression similar to (2.4.1), where all factors fulfill (2.2.10), (2.2.11) and (2.2.12). On the other hand, the state $\rho_{sep} = |00\rangle\langle 00|$ has the local decomposition

$$\rho_{sep} = \frac{1}{4}(\mathbb{I} \otimes \mathbb{I} + \mathbb{I} \otimes \sigma_z + \sigma_z \otimes \mathbb{I} + \sigma_z \otimes \sigma_z) = \frac{1}{2}(\mathbb{I} + \sigma_z) \otimes \frac{1}{2}(\mathbb{I} + \sigma_z),$$

which clearly is separable.
For the general density operator ρ, finding out whether or not the criterion (2.4.1) is fulfilled can be a grueling task, which is why much research has had the aim to find alternate criteria. We will review some of these findings in sections 2.4.3, 2.4.4 and 2.4.5 below.

2.4.2 Bell measurement

To determine the Bell state content of a given two-qubit state ρ, it can be measured in the non-local orthonormal basis

$$\{\Psi_i\}_{i=1}^4, \quad (2.4.5)$$

which gives a projected state

$$\rho \quad \overset{\text{BM}}{\longrightarrow} \quad \rho_p = \sum_{i=1}^{4} \text{Tr}(|\Psi_i\rangle\langle\Psi_i|\rho)|\Psi_i\rangle\langle\Psi_i|. \quad (2.4.6)$$

Observe that generally $\rho \neq \rho_p$. An example of complete Bell measurement can be found in [21].

2.4.3 Bell inequalities

A Bell inequality[5] impose constraints on predicitions of measurements on a physical system so that if the system sustains classical correlations, the inequality is fulfilled. Such inequalities were employed by Bell to discard theories for quantum correlations assuming local realism since these would need additional, Lorentz invariant mechanisms to add the quantum behavior. A variant of the original Bell inequality is the Clauser-Horne-Shimony-Holt (CHSH) inequality[22][2]

$$|\langle A \otimes B\rangle + \langle A \otimes B'\rangle + \langle A' \otimes B\rangle - \langle A' \otimes B'\rangle| \leq 2, \tag{2.4.7}$$

where A, A', B and B' are operators such that the eigenstates of each operator are orthogonal to those of the other operators. A state which violates a Bell inequality evidently exhibits non-classical correlations, in other words, the state is entangled. A common way of writing (2.4.7) is

$$|E(1,1) + E(1,2) + E(2,1) - E(2,2)| \leq 2. \tag{2.4.8}$$

2.4.4 The Positive Partial Transpose criterion

The Positive Partial Transpose (PPT) criterion[23] [24], or Peres-Horodecki criterion, states that a state ρ on $\mathcal{H}_C = \mathcal{H}_A \otimes \mathcal{H}_B$, dim$\mathcal{H}_A$=2, dim($\mathcal{H}_B$)=2 or 3, is separable iff

$$\forall |\psi\rangle^C : \ {}^C\langle\psi|\rho^{T_A}|\psi\rangle^C \geq 0 \tag{2.4.9}$$

This gives a simple mechanism to identify separability (entanglement); simply look for a positive (negative) partial transpose.
In higher dimensions the situation is more complicated, and the PPT criterion becomes weaker, stating only that separable states have PPT. Moreover, in higher dimensions the PPT criterion might prove impractical since it requires a full knowledge of the density matrix of the state, something which for e.g. a $2^{\otimes N}$ Hilbert space would require 4^N measurement settings.

2.4.5 Entanglement witnesses

The notion that the separable states form a convex and compact set, together with Hahn-Banach theorem, gives that any inseparable state can be separated[3] from the separable states by a hyperplane[25]. This is visualized in fig. 2.1.
From this follows that for any entangled state there exists an entanglement witness (EW) observable which defines a hyperplane in Hilbert space such that the entangled state is on one side of it, while all separable states are on the other side[24]. Convention has become that the witness shall assign a negative expectation value to the states on same side as the entangled state and a positive semi-definite expectation value to all other.
That is, for an EW $\mathcal{W}$:

$$\mathrm{Tr}(\mathcal{W}\rho) \begin{cases} \geq 0 & \Rightarrow \quad \rho \quad \text{is separable or inseparable} \\ < 0 & \Rightarrow \quad \rho \quad \text{is inseparable} \end{cases}, \tag{2.4.10}$$

[2]Due to its clarity, the "CH74" paper[22] was preferred over the original 1969 paper by Clauser, Horne, Shimony and Holt.
[3]No pun intended.

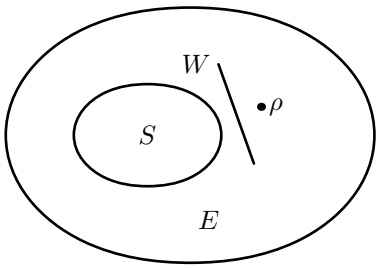

Figure 2.1: The separable states S and a particular entangled state ρ in the set of entangled states E, can be separated by a hyperplane defined by the witness operator W.

so that a negative expectation value always implies entanglement. Fig. 2.1 illustrates the relationships between the separable states, the entangled state and the witness operator. A common flavor of EW is the maximum overlap witness

$$\mathcal{W} = \alpha \mathbb{I}^{\otimes n} - \rho, \tag{2.4.11}$$

for an n-qubit state ρ, where $\alpha = \max\langle \Psi_{sep}|\rho|\Psi_{sep}\rangle$ for all separable states $|\Psi_{sep}\rangle$. For PPT entangled states some tuning of the witness is required [26].
Maximum overlap witnesses can sometimes be tedious to measure due to complex local decompositions, which is why other variants, such as Stabilizer Witnesses [27], have been developed. A stabilizing operator is an operator S_j for which a particular state Ψ is left invariant:

$$S_j \Psi = \Psi. \tag{2.4.12}$$

A stabilizer is a group of such operators, and entanglement witnesses may be formed

$$\mathcal{W} = c_0 \mathbb{I} - \sum_i S_i, \tag{2.4.13}$$

where S_i are stabilizing operators, and

$$c_0 = \max_{\rho \in \mathcal{P}} \langle \sum_i S_i \rangle, \tag{2.4.14}$$

with $\mathcal{P}$ as the set of all separable (n-separable) states. Here, the validity of the entanglement witness depends on the local commutation properties of the stabilizing operators; locally non-commuting operators ensure that there does not exist any separable state giving a negative value of the witness.

2.4.6 Distillability

States ρ_d that are entangled are called *distillable*[12] when it is possible to "distill" maximal entanglement from some number n such states by means of LOCC. That is,

$$\rho_d^{\otimes n} \quad \xrightarrow{\text{LOCC}} \quad \rho_{max}. \tag{2.4.15}$$

The resulting state ρ_{max} has the equivalent amount of entanglement of a singlet state between some of its subspaces.

An undistillable state is impossible to teleport faithfully. Separable states are trivially undistillable since it is impossible to increase the amount of entanglement in a system by LOCC. See [12] for some examples and background on distillation schemes.

2.4.7 Bound entanglement

States that are entangled, yet undistillable, are called bound entangled (BE) states. It has been shown in [28] that a positive partial transpose (PPT) over a certain cut implies undistillability over said cut. This is why there has been some effort to theoretically characterize families of entangled states that have PPT over some cut, while being entangled over this cut. Indeed, such states exist, Acín et al. [29] give a family of tri-partite BE states

$$\rho_b \doteq \frac{1}{n}\begin{pmatrix} 1 & 0 & 0 & 0 & 0 & 0 & 0 & 1 \\ 0 & a & 0 & 0 & 0 & 0 & 0 & 0 \\ 0 & 0 & b & 0 & 0 & 0 & 0 & 0 \\ 0 & 0 & 0 & c & 0 & 0 & 0 & 0 \\ 0 & 0 & 0 & 0 & \frac{1}{c} & 0 & 0 & 0 \\ 0 & 0 & 0 & 0 & 0 & \frac{1}{b} & 0 & 0 \\ 0 & 0 & 0 & 0 & 0 & 0 & \frac{1}{a} & 0 \\ 1 & 0 & 0 & 0 & 0 & 0 & 0 & 1 \end{pmatrix}, \tag{2.4.16}$$

$a, b, c > 0$ and $n = 2 + a + b + c + 1/c + 1/b + 1/a$, for which an entanglement witness and a scheme of production was presented in Hyllus et al.[30].
Also notable is the family of BE states of Horodecki et al. [31]

$$\rho_b \doteq \frac{1}{7b+1}\begin{pmatrix} b & 0 & 0 & 0 & 0 & b & 0 & 0 \\ 0 & b & 0 & 0 & 0 & 0 & b & 0 \\ 0 & 0 & b & 0 & 0 & 0 & 0 & b \\ 0 & 0 & 0 & b & 0 & 0 & 0 & 0 \\ 0 & 0 & 0 & 0 & \frac{1+b}{2} & 0 & 0 & \frac{\sqrt{1-b^2}}{2} \\ b & 0 & 0 & 0 & 0 & b & 0 & 0 \\ 0 & b & 0 & 0 & 0 & 0 & b & 0 \\ 0 & 0 & b & 0 & \frac{\sqrt{1-b^2}}{2} & 0 & 0 & \frac{1+b}{2} \end{pmatrix}, \tag{2.4.17}$$

$0 < b < 1$, which have a PPT, but can be shown to be entangled.
The Smolin state[13], with which the present paper is concerned, is bound entangled but has *unlockable* entanglement. It does not, however, have the "simultaneous PPT and entanglement" property of the states above. This state is described in more detail in chapter 3.

2.5 Quantum Gates

Quantum gates are simple canonical unitary, and thus reversible, operators that can be used to produce more complex quantum circuits with well defined outputs[32].

2.5.1 The Hadamard gate

The *Hadamard gate* operates on a single qubit and rotates it

$$H = \frac{1}{\sqrt{2}}\left(\left(|0\rangle + |1\rangle\right)\langle 0| + \left(|0\rangle - |1\rangle\right)\langle 1|\right), \tag{2.5.1}$$

It can be represented by the matrix

$$H \doteq \frac{1}{\sqrt{2}} \begin{pmatrix} 1 & 1 \\ 1 & -1 \end{pmatrix}. \tag{2.5.2}$$

Fig. 2.2 shows the symbol for the Hadamard gate.

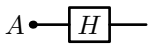

Figure 2.2: A Hadamard gate acting on the qubit A.

2.5.2 The CNOT gate

The *Controlled NOT gate* operates on two qubits A and B and flips B if A is $|1\rangle$

$$CNOT_{AB} = |00\rangle^{AB}\langle 00| + |01\rangle^{AB}\langle 01| + |10\rangle^{AB}\langle 11| + |11\rangle^{AB}\langle 10|, \tag{2.5.3}$$

Its matrix representation is

$$CNOT \doteq \begin{pmatrix} 1 & 0 & 0 & 0 \\ 0 & 1 & 0 & 0 \\ 0 & 0 & 0 & 1 \\ 0 & 0 & 1 & 0 \end{pmatrix}. \tag{2.5.4}$$

Fig. 2.3 shows the symbol for the CNOT gate.

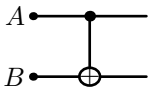

Figure 2.3: A CNOT gate acting on the qubits A and B.

2.5.3 The controlled phase flip gate

The *Controlled Phase flip gate* operates on two qubits A and B and flips the phase of B π radians if A is $|1\rangle$.

$$P = |00\rangle^{AB}\langle 00| + |01\rangle^{AB}\langle 01| + |10\rangle^{AB}\langle 10| - |11\rangle^{AB}\langle 11|, \tag{2.5.5}$$

with the matrix representation

$$P \doteq \begin{pmatrix} 1 & 0 & 0 & 0 \\ 0 & 1 & 0 & 0 \\ 0 & 0 & 1 & 0 \\ 0 & 0 & 0 & -1 \end{pmatrix}. \tag{2.5.6}$$

This is a special case of the Controlled Phase gate, but for our purposes this will suffice. Fig. 2.4 shows the symbol for the Controlled Phase Flip gate.

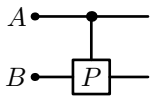

Figure 2.4: A Controlled Phase Flip gate acting on the qubits A and B.

2.6 Photonic Systems

The Hamiltonian for photons propagating in a mode i is the quantum mechanical harmonic oscillator [17]

$$H = \hbar\omega(a_i^\dagger a_i + 1/2), \tag{2.6.1}$$

where

$$[a_i, a_i^\dagger] = 1. \tag{2.6.2}$$

This Hamiltonian has orthonormal eigenstates $|n_i\rangle$ with corresponding eigenvalues $E_{n_i} = \hbar\omega(n_i + 1/2)$, where the number n_i corresponds to the number of photons in mode i. The eigenstates satisfy

$$a_i|n_i\rangle = \sqrt{n_i}|n_i - 1\rangle, \tag{2.6.3}$$

and

$$a_i^\dagger|n_i\rangle = \sqrt{n_i + 1}|n_i + 1\rangle. \tag{2.6.4}$$

Since the operator a_i ($a_i^\dagger$) can be said to annihilate (create) a quantum of energy in the harmonic oscillator, the name annihilation (creation) operator is appropriate. Again, in a photonic system, the annihilation and creation of quanta corresponds to the annihilation and creation of photons.
For photons it will be useful to denote the polarization mode along with the spatial mode of the photons, an annihilation (creation) operator for spatial mode i and polarization mode j will consequently be denoted $a_{ij}^{(\dagger)}$. Occasionally additional mode information may be appended to the subscript.
A qubit in spatial mode i can be encoded on a photon as

$$|0\rangle^i \doteq |v_i\rangle \equiv |1_{iv}\rangle = a_{iv}^\dagger|0_{iv}\rangle \tag{2.6.5}$$

$$|1\rangle^i \doteq |h_i\rangle \equiv |1_{ih}\rangle = a_{ih}^\dagger|0_{ih}\rangle. \tag{2.6.6}$$

2.6.1 Beam splitters

The general beam splitter[33] (GBS) operates on incoming photons in two spatial modes 1 and 2 (See fig. 2.5)
and transforms it to outgoing photons in the same modes according to

$$a_{1v}^\dagger \to t_{1v}a_{1v}^\dagger + ir_{1v}a_{2v}^\dagger$$

$$a_{1h}^\dagger \to t_{1h}a_{1h}^\dagger + ir_{1h}a_{2h}^\dagger$$

$$a_{2v}^\dagger \to t_{2v}a_{2v}^\dagger + ir_{2v}a_{1v}^\dagger$$

$$a_{2h}^\dagger \to t_{2h}a_{2h}^\dagger + ir_{2h}a_{1h}^\dagger,$$

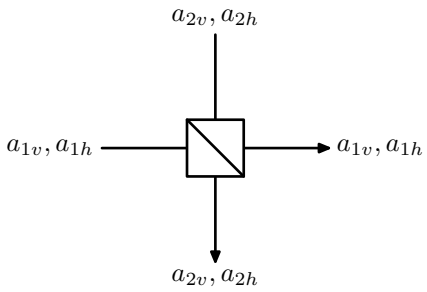

Figure 2.5: General beam splitter operating on the spatial modes 1 and 2.

where t_{ij}^2 is the probability density of a photon in spatial mode i to be transmitted in this same mode, keeping its polarization j and r_{ij}^2 is the probability density of a photon being reflected from spatial mode i to the other spatial mode, also keeping its polarization.
Its matrix representation is

$$S_{GBS} = \begin{pmatrix} t_{1v} & 0 & ir_{2v} & 0 \\ 0 & t_{1h} & 0 & ir_{2h} \\ ir_{1v} & 0 & t_{2v} & 0 \\ 0 & ir_{1h} & 0 & t_{2h} \end{pmatrix}. \tag{2.6.7}$$

To obtain the matrix description of the GBS we have introduced the operator basis below for the two spatial and the two polarization modes.

$$a_{1v} \doteq \begin{pmatrix} 1 \\ 0 \\ 0 \\ 0 \end{pmatrix} a_{1h} \doteq \begin{pmatrix} 0 \\ 1 \\ 0 \\ 0 \end{pmatrix} a_{2v} \doteq \begin{pmatrix} 0 \\ 0 \\ 1 \\ 0 \end{pmatrix} a_{2h} \doteq \begin{pmatrix} 0 \\ 0 \\ 0 \\ 1 \end{pmatrix} \tag{2.6.8}$$

To maintain unitarity of the GBS, the r's and t's must satisfy $t_i^2 + r_i^2 = 1$, for $i \in \{1v, 1h, 2v, 2h\}$ and $t_{1i}r_{2i} - t_{2i}r_{1i} = 0$, where $i \in \{v, h\}$.
There are two common specializations of the GBS, the symmetric beamsplitter (BS) and the polarizing beamsplitter (PBS), their respective constraints and operations are given below.

The symmetric beam splitter

The operation of the symmetric beam splitter:

$$t_i = r_i = \tfrac{1}{\sqrt{2}}, i \in \{1v, 1h, 2v, 2h\} \quad \Rightarrow \quad \begin{cases} a_{1v}^\dagger \to \frac{1}{\sqrt{2}}(a_{1v}^\dagger + ia_{2v}^\dagger) \\ a_{1h}^\dagger \to \frac{1}{\sqrt{2}}(a_{1h}^\dagger + ia_{2h}^\dagger) \\ a_{2v}^\dagger \to \frac{1}{\sqrt{2}}(a_{2v}^\dagger + ia_{1v}^\dagger) \\ a_{2h}^\dagger \to \frac{1}{\sqrt{2}}(a_{2h}^\dagger + ia_{1h}^\dagger) \end{cases}$$

whose matrix representation is

$$S_{BS} = \frac{1}{\sqrt{2}} \begin{pmatrix} 1 & 0 & i & 0 \\ 0 & 1 & 0 & i \\ i & 0 & 1 & 0 \\ 0 & i & 0 & 1 \end{pmatrix}. \tag{2.6.9}$$

The polarizing beam splitter

The operation of the polarizing beamsplitter:

$$t_{iv} = r_{ih} = 1, t_{ih} = r_{iv} = 0, i \in \{1,2\} \quad \Rightarrow \quad \begin{cases} a^\dagger_{1v} \to a^\dagger_{1v} \\ a^\dagger_{1h} \to i a^\dagger_{2h} \\ a^\dagger_{2v} \to a^\dagger_{2v} \\ a^\dagger_{2h} \to i a^\dagger_{1h} \end{cases}$$

whose matrix representation is

$$S_{PBS} = \begin{pmatrix} 1 & 0 & 0 & 0 \\ 0 & 0 & 0 & i \\ 0 & 0 & 1 & 0 \\ 0 & i & 0 & 0 \end{pmatrix}. \tag{2.6.10}$$

2.6.2 Wave plates

Wave plates[33] are birefringent crystals that can be used to manipulate the polarization of photons by delaying one polarization component, i.e. shifting, or retarding, their phase.

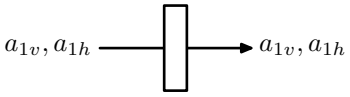

Figure 2.6: General wave plate operating on spatial mode 1.

For a general WP of thickness d, the phase retardation is given by

$$2\pi c = 2\pi(c_0 + m) = \frac{2\pi \Delta n \; d}{\lambda}, \qquad c_0 \in [0,1[\quad , \quad m \in \mathbb{Z}_+ \tag{2.6.11}$$

where the *birefringence* $\Delta n = n_{slow} - n_{fast}$, i.e. the difference in refractive indices of the slow and the fast axes of the crystal. $2\pi c_0$ is the zero-order retardation and the term m corresponds to the full-wave phase shifts added when using a crystal thicker than $d = \lambda/\Delta n$. The unitary operation of a general wave plate on photons in spatial mode j is:

$$\begin{aligned} a^\dagger_{jv} \quad &\to \quad (e^{-2\pi ci}\cos^2\phi + \sin^2\phi)\, a^\dagger_{jv} \quad + \quad \tfrac{1}{2}(1 - e^{-2\pi ci})\sin(2\phi)\, a^\dagger_{jh} \\ a^\dagger_{jh} \quad &\to \quad \tfrac{1}{2}(1 - e^{-2\pi ci})\sin(2\phi)\, a^\dagger_{jv} \quad + \quad (\cos^2\phi + e^{-2\pi ci}\sin^2\phi)\, a^\dagger_{jh} \end{aligned}$$

Here, ϕ is the angle from the fast axis of the WP to the vertical polarization plane. Its matrix representation is

$$S_{cWP} = \begin{pmatrix} e^{-2\pi ci}\cos^2\phi + \sin^2\phi & \frac{1}{2}(1-e^{-2\pi ci})\sin 2\phi \\ \frac{1}{2}(1-e^{-2\pi ci})\sin 2\phi & \cos^2\phi + e^{-2\pi ci}\sin^2\phi \end{pmatrix} \tag{2.6.12}$$

Since the waveplate has only one spatial mode, with two polarization modes, the basis of the matrix is reduced to:

$$a_{1v} \doteq \begin{pmatrix} 1 \\ 0 \end{pmatrix} a_{1h} \doteq \begin{pmatrix} 0 \\ 1 \end{pmatrix}.$$

The operation of the WP can be specialized to the cases where $c = \frac{1}{2} + n\lambda$ and $c = \frac{1}{4} + n\lambda$, $n \in \mathbb{Z}$, which correspond to a half-wave plate (HWP) and a quarter-wave plate (QWP) respectively. Their operations on photons in mode j are given below.

The half-wave plate

Operation of the half-wave plate

$$\begin{array}{rcccc} a_{jv}^\dagger & \to & (\sin^2\phi - \cos^2\phi)\, a_{jv}^\dagger & + & \sin(2\phi)\, a_{jh}^\dagger \\ a_{jh}^\dagger & \to & \sin(2\phi)\, a_{jv}^\dagger & + & (\cos^2\phi - \sin^2\phi)\, a_{jh}^\dagger \end{array},$$

its matrix representation

$$S_{HWP} = \begin{pmatrix} \sin^2\phi - \cos^2\phi & \sin 2\phi \\ \sin 2\phi & \cos^2\phi - \sin^2\phi \end{pmatrix}$$

The quarter-wave plate

Operation of the quarter-wave plate

$$\begin{array}{rcccc} a_{jv}^\dagger & \to & (\sin^2\phi - i\cos^2\phi)\, a_{jv}^\dagger & + & \frac{1}{2}(1+i)\sin(2\phi)\, a_{jh}^\dagger \\ a_{jh}^\dagger & \to & \frac{1}{2}(1+i)\sin(2\phi)\, a_{jv}^\dagger & + & (\cos^2\phi - i\sin^2\phi)\, a_{jh}^\dagger. \end{array}$$

and its matrix representation

$$S_{QWP} = \begin{pmatrix} \sin^2\phi - i\cos^2\phi & \frac{1}{2}(1+i)\sin 2\phi \\ \frac{1}{2}(1+i)\sin 2\phi & \cos^2\phi - i\sin^2\phi \end{pmatrix}.$$

Wave plates as phase shifts

A wave plate may be employed as a variable phase shift by varying the length photons travel through it. One variation on this theme is to fix $\phi = 0$ and then tilt the wave plate an angle θ around the slow axis. Since the length the photons will travel through the crystal (disregarding the effects of refraction etc.) now is $d' = d/\cos(\theta)$, the phase shift is changed. By (2.6.11), $c' = c/\cos(\theta)$. This gives the operation

$$\begin{array}{rcl} a_{jv}^\dagger & \to & e^{-2\pi c' i}\, a_{jv}^\dagger = e^{\frac{-2\pi ci}{\cos\theta}}\, a_{jv}^\dagger \\ a_{jh}^\dagger & \to & a_{jh}^\dagger \end{array}.$$

with the matrix representation

$$S_{c\theta WP} = \begin{pmatrix} e^{\frac{-2\pi ci}{\cos\theta}} & 0 \\ 0 & 1 \end{pmatrix}$$

2.6.3 Non-linear optics

The polarization density in a crystal can be expanded in a power series

$$P_i = \varepsilon_0 \left(\chi^{(1)}_{ij} E_j + \chi^{(2)}_{ijk} E_j E_k + \chi^{(3)}_{ijkl} E_j E_k E_l ... \right).$$

For linear crystals the higher order susceptibility tensors, such as $\chi^{(2)}_{ijk}$ are negligibly small compared to $\chi^{(1)}_{ij}$ so that linear interactions will dominate. However, for strong fields or high optical non-linearities, the higher order tensors come into play, giving rise to new phenomena. Among these are e.g. *Spontaneous Parametric Down-Conversion* which has become an important tool in quantum optics.

Spontaneous Parametric Down-Conversion

With the contributions of higher order terms, the polarization density can couple one photon to two or more photons. When multiple incoming photons are coupled to produce one outgoing photon the process is referred to as a sum frequency process, and conversely, when one incoming photon is coupled to multiple outgoing photons the process is called a difference frequency process or Spontaneous Parametric Down-Conversion. "Spontaneous" refers to the quantum fluctuations giving rise to the process, while "Parametric" means that the state of the crystal is not altered by the operation. "Down-Conversion" simply means that the frequency of the outgoing photons is less than that of the incoming photon. In order for these processes to take place for the conversion of one photon into two and vice versa, two criteria have to be fulfilled:

$$\mathbf{k}_0 = \mathbf{k_1} + \mathbf{k_2} \tag{2.6.13}$$

$$\omega_0 = \omega_1 + \omega_2, \tag{2.6.14}$$

where the $\mathbf{k}_i$ are the wave vectors and the ω_i the angular frequencies of the photons. The criteria are recognized as the preservation of momentum and the preservation of energy respectively.
Type I processes are those where the two photons share the same polarization, where in type II processes they have opposite polarization.

Crystals that exhibit high non-linearities include e.g. LBO (LiB_3O_4) and BBO (β-BaB_2O_4). The crystal can be cut to accommodate either type I or type II processes. In the case of two photon SPDC, a single type II crystal can be used directly with an unpolarized laser **[?]** (in mode i) to produce a $|\Psi^+\rangle$ (in modes j and k), consequently,

$$a^\dagger_i \overset{\text{Type II}}{\longrightarrow} a^\dagger_{jh} a^\dagger_{kv} - a^\dagger_{jv} a^\dagger_{kh}. \tag{2.6.15}$$

The modes j and k are taken to be located in the intersections between the extraordinary and the ordinary light cones on the output side of the crystal.

The type I crystal, however, outputs pairs of equally polarized photons (into modes j and k) of polarization opposite to that of the beam (mode i),

$$\begin{aligned} a_{iv}^{\dagger} &\overset{\text{Type I}}{\longrightarrow} a_{jh}^{\dagger} a_{kh}^{\dagger} \\ a_{ih}^{\dagger} &\overset{\text{Type I}}{\longrightarrow} a_{jv}^{\dagger} a_{kv}^{\dagger}. \end{aligned} \tag{2.6.16}$$

Here, the output modes j and k occur anywhere around a cone on the output side of the crystal, although always at diametrally opposed positions, due to eqs. (2.6.13) and (2.6.14). As a result, $|\Phi^+\rangle$ can be obtained by pumping two stacked type I BBO's with a laser of $a_{iv}^{\dagger} + a_{ih}^{\dagger}$ polarization. For the purpose of producing polarization entangled photons the type II crystal has been the most frequently used, although it has been shown [34] that type I crystals can produce sources for entanglement several orders of magnitude brighter.

CHAPTER 3

THE SMOLIN STATE

It's not stupid, it's advanced.
- T. T.

3.1 Properties of the Smolin state

Smolin [13] found that a mixture of Bell states

$$\rho_S^{ABCD} = \frac{1}{4}\sum_{i=1}^{4} |\Psi_i\rangle^{AB}\langle\Psi_i| \otimes |\Psi_i\rangle^{CD}\langle\Psi_i|, \tag{3.1}$$

where $\{|\Psi_i\rangle\}_{i=1}^4 = \{|\Psi^-\rangle, |\Psi^+\rangle, |\Phi^+\rangle, |\Phi^-\rangle\}$, produces an entangled state which is not distillable, i.e. bound entangled, but which is possible to "unlock" to a distillable configuration.
This state is somewhat different from previous examples of bound entangled states in section 2.4.7. It does not have a PPT over a cut where it is also entangled, but rather one have to envision that the bound entanglement comes from it being separable at every partition that separates two parties from the other two. Only by bringing together any two parties, or *unlocking* the state, is it possible to distill maximal entanglement from it. It seems questionable if bound entanglement of the Smolin state stems from the same phenomenon as for the PPT entangled states of section 2.4.7. The matrix representation of the Smolin state density is shown in fig. 3.1, revealing its remarkable symmetry.

A second way of writing the Smolin state is as a combination of GHZ-states,

$$\rho_S^{ABCD} = \frac{1}{4}\sum_{i=1}^{4} |\Psi_i^{GHZ}\rangle^{ABCD}\langle\Psi_i^{GHZ}|, \tag{3.2}$$

where

$$[|\Psi_i^{GHZ}\rangle]_{i=1}^4 = \big[\tfrac{1}{\sqrt{2}}(|0000\rangle + |1111\rangle), \tfrac{1}{\sqrt{2}}(|1100\rangle + |0011\rangle), \tfrac{1}{\sqrt{2}}(|1010\rangle + |0101\rangle), \tfrac{1}{\sqrt{2}}(|1001\rangle + |0110\rangle)\big].$$

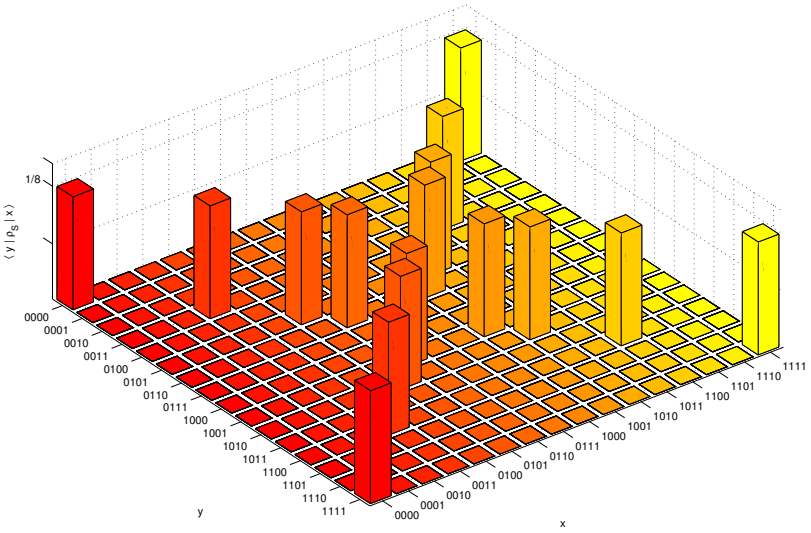

Figure 3.1: Matrix representation of the density operator ρ_S of the Smolin state

Each of these GHZ-states correspond to one of the four "squares" in the density matrix, as seen in fig. 3.1. Finally, a third way of viewing the Smolin state is as its local decomposition

$$\rho_S^{ABCD} = \frac{1}{16}\sum_{i=1}^{4}\sigma_i^{\otimes 4}, \tag{3.3}$$

where $\{\sigma_i\}_{i=1}^4 = \{\mathbb{I}, \sigma_x, \sigma_y, \sigma_z\}$. All these three versions of the Smolin state all seem peculiarly symmetric and simple, which is going to be a great help when trying generate or analyze the state in reality.

Here is a summary of the properties of the Smolin state.

1. Symmetry under interchange of parties. This can easiest be seen from the local decomposition (3.3). Switching any two factors of any term does not affect the state. The symmetry property is explored to some extent in section 3.3.5.

2. Entanglement. The state violates the PPT criterion at the cut A|BCD, since

$$\rho_S{}^{T_A}|\psi\rangle = \lambda|\psi\rangle \Rightarrow min\ \lambda < 0 \tag{3.4}$$

   and given the symmetry property, it does so in every partition where one party is separated from the other three i.e. in every 1|3 partition. This also rules out separability in the finer cases of the 1|1|2 and 1|1|1|1 partitions.
   A Bell inequality and two entanglement witnesses are given in sections 3.3.1, 3.3.2 and 3.3.3, providing further proof of the entanglement of ρ_S.

3. Non-distillability. Every party is separated from every other across a separable cut [35]. This property follows from the facts that the state is separable across the cut AB|CD by construction and that it has the symmetry property above, giving separability in every 2|2 cut. Since no entanglement can be distilled across a separable cut, the state is non-distillable.

Separation	Cut	Distillability
A|B|C|D	A|BCD	Not distillable, "locked" configuration
A|B|CD	A|BCD	Distillable, "unlocked", altruistic configuration
A|BCD	A|BCD	Distillable
A|B|CD	AB|CD	Not distillable, separable cut
AB|CD	AB|CD	Not distillable, separable cut

Figure 3.2: Distillability summary. ”Separation” shows how the four parties are separated, i.e. parties not separated by a ”|” are considered local, thus capable of performing Bell measurements. ”Cut” refers to the cut over which entanglement distillation is attempted. ”Distillability” shows the success/failure of the distillation. Permutations of A, B, C and D does not affect the distillability.

4. Unlockability. The entanglement of the state can be unlocked by bringing two parties together since these parties can perform a Bell-measurement to determine which Bell state they had and communicate the results to the other parties which then will share the same pure Bell-state.

It is worth mentioning that there are no states in lower dimensions than $2^{\otimes 4}$ that have properties similar to ρ_S^{ABCD}, although Augusiak and Horodecki [36] have generalized the concept of the Smolin state to higher dimensions.
The plethora of exotic features of the Smolin state motivates further study. Below are presented four approaches to producing the Smolin state.

3.2 Generation of the Smolin state

The Smolin state admits generation in a variety of ways, however, all approaches must involve the mixing of several pure states. Below are presented three setups based on quantum gates, producing the Smolin state starting from an all zero state, two Bell states and a GHZ state respectively. These setups require six qubits to get the desired result, discarding two of these in the mixing process. Although these setups are general in the sense that they do not have features endemic to any particular technology, reproducing these in a purely photonic framework will be difficult. Hence, a fourth solution is proposed. This solution uses four qubits encoded on four photons and relies on a ”manual” mixture of the pure states initially produced.

3.2.1 A network of quantum gates, starting from an all-zero state

The first setup, using fundamental quantum gates to produce ρ_S^{ABCD}, is similar to the one presented for the Acín et al. state [29] in Hyllus et al. [30] First there is a preparation

stage where four qubits for the ρ_S^{ABCD} and the ancillae are prepared, followed by a modification stage where the ancillae interact with the state qubits and finally a trace-out of the ancillae. All in all this requires 7 CNOT-gates, 3 Hadamard-gates and six qubits including the ancillae. These resources compare well to those of e.g. Hyllus et al.

Presented below is a diagram over the quantum network used to obtain the Smolin state.

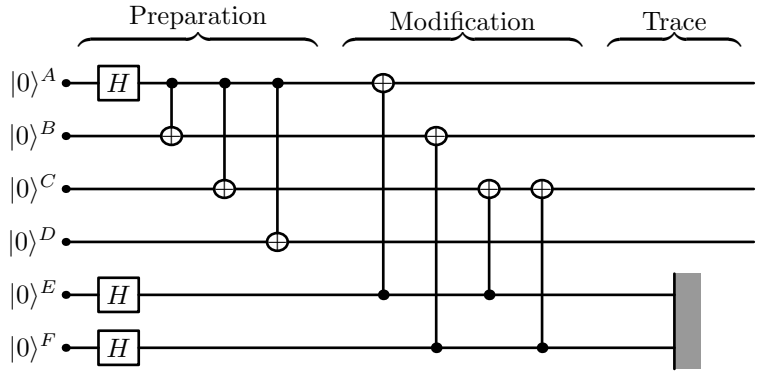

Figure 3.3: Setup 1: Quantum network for the Smolin state

Noting that the Smolin state can be written as a combination of four 4-party GHZ states as follows,

$$\rho_S^{ABCD} = \frac{1}{4}\sum_{i=1}^{4} |\Psi_i^{GHZ}\rangle^{ABCD}\langle\Psi_i^{GHZ}|, \tag{3.2.1}$$

where

$$[|\Psi_i^{GHZ}\rangle]_{i=1}^4 = \big[\tfrac{1}{\sqrt{2}}(|0000\rangle + |1111\rangle), \tfrac{1}{\sqrt{2}}(|1100\rangle + |0011\rangle), \\ \tfrac{1}{\sqrt{2}}(|1010\rangle + |0101\rangle), \tfrac{1}{\sqrt{2}}(|1001\rangle + |0110\rangle)\big],$$

the stategy of the setup is to produce all $|\Psi_i^{GHZ}\rangle$, and couple each of these to a specific ancilla configuration. This will give ρ_S^{ABCD} as the sum (3.2.1) upon tracing out the ancillae. The calculation is described in section A.1.

3.2.2 A network of quantum gates, starting from a GHZ-state

Should the experimental setup provide a four-partite GHZ-state initially, the preparation stage of setup 1 can be largely omitted, resulting in a second simplified setup:

3.2.3 A network of quantum gates, starting from two bell states

Some sources of entanglement readily provide EPR-pairs, from which the Smolin state can be produced by a third setup presented in fig. 3.5. The stategy of the setup is to produce all $|\Psi_i\rangle$, by flipping qubits and shifting phases while coupling each these to a specific ancilla configuration. This will give ρ_S^{ABCD} upon tracing out the ancillae.
Note that the setup is independent of which EPR-pair is used initially.

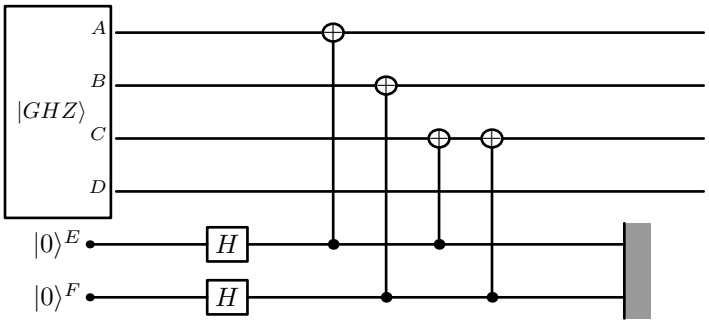

Figure 3.4: Setup 2: Quantum network for the Smolin state, starting from a four-partite GHZ-state.

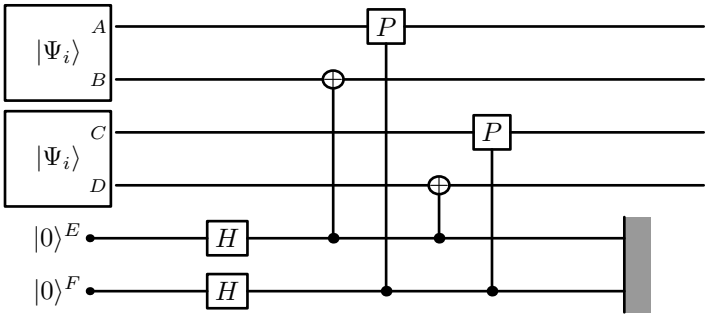

Figure 3.5: Setup 3: Quantum network for the Smolin state, starting from two EPR-pairs

3.2.4 A photonic system

Below is presented a photonic setup which is specifically designed to avoid use of the immense resources (currently) required to produce one of the setups above in a photonic regime. This setup is based on a standard pulsed Type-II SPDC source of entangled photons, which is employed to produce Bell-pairs. The remainder of the setup is quite similar to setup 3 above in the sense that it takes two identical Bell states and randomly flips the state and phase of the qubits, producing a symmetric mixture of all the Bell states, the Smolin state. The pivotal difference is that the purely photonic setup uses "manual" mixing of the Bell states.
Here follows an outline of the process, for the full calculation, see appendix A.4 on page 48.

Stage 1, Production of a Bell State: The pump laser (see fig. 3.6) produces a polarization entangled photon pair in $|\Psi^+\rangle$ when it impinges on the BBO.

Stage 2, Transformation to an Arbitrary Bell State: The filters F1 and F2 increase the decoherence length of the photons so that they become more suitable for coincidence measurement. The entangled state meets the quarter-wave plate QWP1, which is oriented with its fast axis parallel to the vertical axis. By tilting QWP1 around an axis perpendicular to the incident light, the difference in optical path length gives tunable shifts in phase. Thus the phase of the state can be adjusted to either +1 or

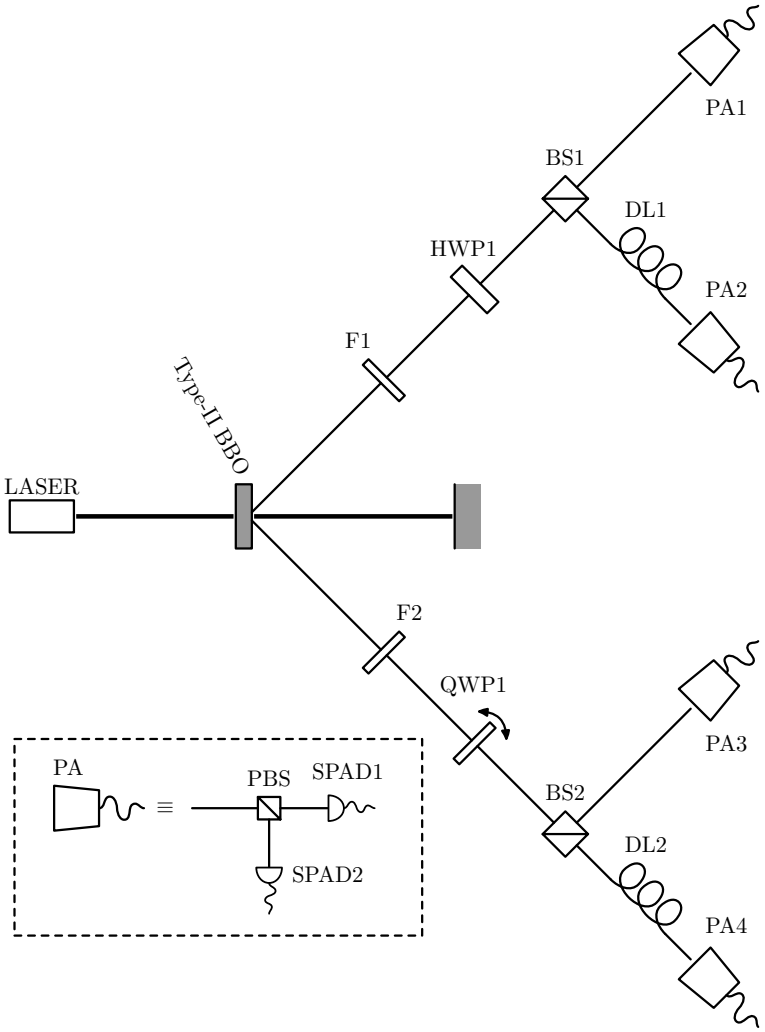

Figure 3.6: A photonic setup for the Smolin state, where a laser impinges on a Type-II BBO crystal, producing an entangled pair of photons which passes through the filters F1 and F2 to increase its coherence length. QWP1 is either set to leave the state unchanged or flip its phase. HWP1 is either set to leave the state unchanged or flip the polarization of one of the photons. The beam splitters BS1 and BS2 distribute each of the photons either directly to the polarization analyzers PA1 and PA3, or via the delay lines DL1, DL2 to PA2 and PA4.

-1.

HWP1 has two settings: either flip one bit of the entangled state, or leave it untouched. QWP1 and HWP2 together makes it possible to produce all four Bell-states.

Stage 3, Mixing of Two Bell States The two beam splitters BS1 and BS2 distribute incident photons either to the delay line (DL1 or DL2 respectively) or to the branch that goes directly to the detectors. This gives the probability $\frac{1}{4}$ that both photons from a given down-conversion go into the delay lines. The same probability is valid for the case where the two photons go directly to the detectors. Since the laser is

operated in pulsed mode the photons in both of these cases come from the same pulse. The length of the delay lines is such that it compensates for the time between consecutive laser pulses. The case where the photons of a laser pulse go into the delay lines, while the photons from the following pulse go directly to the detectors, will yield a fourfold coincidence at the detectors. This occurs with a probability of $\frac{1}{16}$.

Now, keeping the settings for QWP1 and HWP2 constant until a fourfold coincidence is registered at the detectors will yield one of the states: $|\Phi^+\rangle^{\otimes 2}$, $|\Phi^-\rangle^{\otimes 2}$, $|\Psi^+\rangle^{\otimes 2}$, $|\Psi^-\rangle^{\otimes 2}$. Randomly re-adjusting the settings after the coincidence will produce each of the states above with equal probability, giving ρ_S^{ABCD} at the detectors.

3.3 Analysis of the Smolin state

Once ρ_S^{ABCD} has been produced follows the work to verify its characteristic features, such as entanglement, undistillability, unlockability, symmetry under interchange of parties, and maximal entanglement. Here is proposed a scheme that might be useful in this work.

3.3.1 Bell inequality

Augusiak and Horodecki gave a CHSH-type Bell inequality for the Smolin state in [35]. The inequality is

$$|E(1,1,1,1) + E(1,1,1,2) + E(2,2,2,1) - E(2,2,2,2)| \leq 2. \tag{3.3.1}$$

Evaluating the inequality with

$$O_{1111} = \sigma_x \otimes \sigma_x \otimes \sigma_x \otimes \frac{1}{\sqrt{2}}(\sigma_x + \sigma_z) \tag{3.3.2}$$

$$O_{1112} = \sigma_x \otimes \sigma_x \otimes \sigma_x \otimes \frac{1}{\sqrt{2}}(\sigma_x - \sigma_z) \tag{3.3.3}$$

$$O_{2221} = \sigma_z \otimes \sigma_z \otimes \sigma_z \otimes \frac{1}{\sqrt{2}}(\sigma_x + \sigma_z) \tag{3.3.4}$$

$$O_{2222} = \sigma_z \otimes \sigma_z \otimes \sigma_z \otimes \frac{1}{\sqrt{2}}(\sigma_x - \sigma_z) \tag{3.3.5}$$

$$\begin{aligned} \Rightarrow \quad & |E(1,1,1,1) + E(1,1,1,2) + E(2,2,2,1) - E(2,2,2,2)| \\ & = |\mathrm{Tr}\left((O_{1111} + O_{1112} + O_{2221} - O_{2222})\rho_S\right)| = 2\sqrt{2}, \end{aligned} \tag{3.3.6}$$

which clearly is a violation of the inequality. The state is maximally entangled in the sense that it exhibits the same degree of violation of the Bell inequality as would a Bell state or GHZ state.

3.3.2 Entanglement witness

To rule out triseparability for the biseparable Smolin state the following witness is constructed.

$$\mathcal{W}_S = \alpha \mathbb{I}^{\otimes 4} - \rho_S, \tag{3.3.7}$$

where $\alpha = \max\langle\Psi_{tri}|\rho_S|\Psi_{tri}\rangle$ for all tripartite states $|\Psi_{tri}\rangle$. This maximum occurs for e.g. $|\Psi_{tri}\rangle = |0\rangle|0\rangle|\Phi^+\rangle$ and turns out be $\alpha = \frac{1}{8}$. The resulting witnesses has four eigenvalues $-\frac{1}{8}$ and twelve at $\frac{1}{8}$ and a local decomposition

$$\mathcal{W}_S = \frac{1}{16}(\mathbb{I}^{\otimes 4} - \sigma_x^{\otimes 4} - \sigma_y^{\otimes 4} - \sigma_z^{\otimes 4}), \tag{3.3.8}$$

from which it follows that it can be measured in 3 measurement settings. The expectation value of $\mathcal{W}_S$ for ρ_S is

$$\langle\mathcal{W}_S\rangle_{\rho_S} = -\frac{1}{8} \tag{3.3.9}$$

Since $\mathcal{W}_S$ has multiple negative eigenvalues it must give negative values for other states than the Smolin state. For example

$$\langle\mathcal{W}_S\rangle_{\Psi_i} = -\frac{1}{8}. \tag{3.3.10}$$

Noise tolerance

Mixing the Smolin state with the completely depolarized state, or white noise state, $\rho_{noise} = \frac{1}{16}\mathbb{I}^{\otimes 4}$ gives the noisy state

$$\rho_{Sn} = \frac{p}{16}\mathbb{I}^{\otimes 4} + (1-p)\rho_S, \quad p \in [0,1] \tag{3.3.11}$$

The noise tolerance is the largest p for which the criterium

$$\langle\mathcal{W}_S\rangle_{\rho_{Sn}} < 0 \tag{3.3.12}$$

is valid. This is the maximum amount of white noise for which detection of entanglement is possible. Solving for p gives $p = \frac{2}{3}$. This is also the maximum amount of white noise tolerable by any witness for the Smolin state, since above this limit the Smolin state ceases to be entangled[35].

3.3.3 Entanglement witness in stabilizer formalism

Above, the witness $\mathcal{W}_S$ was treated as a maximum overlap witness, but it can just as easily be seen as a stabilizer witness as those of Tóth and Gühne[27] (see section 2.4.5). The operators $S_x = \sigma_x^{\otimes 4}$ and $S_z = \sigma_z^{\otimes 4}$ are easily seen to be stabilizing operators of the Smolin state, since

$$\sigma_x^{\otimes 4}\rho_S = \sigma_z^{\otimes 4}\rho_S = \rho_S. \tag{3.3.13}$$

It is evident from the local decomposition of the Smolin state (3.3) that these two operators indeed form a complete stabilizer, because the other possible stabilizing operators $\sigma_y^{\otimes 4}$ and $\mathbb{I}^{\otimes 4}$ can be formed as products of the earlier two. As required for a stabilizer for witnesses, these operators are locally non-commuting. However, with respect to 2:2 partitions they do commute:

$$[\,\sigma_z^{\otimes 2},\, \sigma_x^{\otimes 2}\,] = (i\sigma_y)^{\otimes 2} - (-i\sigma_y)^{\otimes 2} = 0. \tag{3.3.14}$$

This simply means that the witness will not be able rule out biseparability of the Smolin state, but the objective here is to rule out triseparability, so we proceed.

A stabilizer witness ruling out full separability can be formed by

$$\mathcal{W}'_S = c_0 \mathbb{I}^{\otimes 4} - S_x - S_z - S_x S_z, \tag{3.3.15}$$

where

$$c_0 = \max_{\rho \in \mathcal{P}} \langle S_x + S_z \rangle, \tag{3.3.16}$$

and $\mathcal{P}$ denotes the set of all separable states. To rule out triseparablility, c_0 would be maximum over the set of triseparable states. It turns out both maxima coincide at $c_0 = 1$ for e.g. $|\Psi_{sep}\rangle = |0\rangle|0\rangle|0\rangle|0\rangle$ and $|\Psi_{tri}\rangle = |0\rangle|0\rangle|\Phi^+\rangle$. Thus, the resulting witness is

$$\mathcal{W}'_S = \mathbb{I}^{\otimes 4} - S_x - S_z - S_x S_z = \mathbb{I}^{\otimes 4} - \sigma_x^{\otimes 4} - \sigma_y^{\otimes 4} - \sigma_z^{\otimes 4}, \tag{3.3.17}$$

which is recognized as the witness from section 3.3.2 without the constant factor. Obviously its noise tolerance is the same. The last $S_x S_z$ term can be dropped to save an analyzer setting when measuring the witness in practice:

$$\mathcal{W}''_S = \mathbb{I}^{\otimes 4} - S_x - S_z \tag{3.3.18}$$

This witness has the slightly lower noise tolerance of $p = \frac{1}{2}$, but it is also the witness that requires the least number of measurements of any possible witness for the Smolin state. This can be seen by noting that removing one more setting would result in

$$\max_{\rho \in \mathcal{P}} \langle S_x \rangle = \max_{\rho \in \mathcal{P}} \langle S_z \rangle = \langle S_x \rangle_{\rho_S} = \langle S_z \rangle_{\rho_S} = 1, \tag{3.3.19}$$

giving useless witnesses of the form $\mathcal{W}'''_S = c_0 \mathbb{I}^{\otimes 4} - S_j$ with $j = x, y, z$.

3.3.4 Measurement and discrimination

From the local decomposition of ρ_S (3.3) it is obvious that the state gives non-zero expectation values when measured in the bases $\sigma_x^{\otimes 4}$, $\sigma_y^{\otimes 4}$ and $\sigma_z^{\otimes 4}$. The expectation values when measuring these observables are

$$\langle \sigma_x^{\otimes 4} \rangle_{\rho_S} = \langle \sigma_y^{\otimes 4} \rangle_{\rho_S} = \langle \sigma_z^{\otimes 4} \rangle_{\rho_S} = 1. \tag{3.3.20}$$

For all other bases the expectation values are zero. To discriminate between ρ_S and a pure state

$$|\Psi_{pure}\rangle = \sum_{i=1}^{4} |\Psi_i\rangle|\Psi_i\rangle$$

as well as other sums of Bell states, the observables $\sigma_i \sigma_i \sigma_j \sigma_j$, $\sigma_i \sigma_j \sigma_j \sigma_i$ and $\sigma_i \sigma_j \sigma_i \sigma_j$, $i, j \in \{0, 1, 2, 3\}$, $i \neq j$, can be measured, since these give zero expectation value with ρ_S but non-zero result with other combinations of Bell states.

3.3.5 Bell state analysis

Analyzing the Bell state content can reveal symmetries in ρ_S. For example all the schemes below should give the same result, thus showing that

$$\begin{aligned} \rho_S &= \tfrac{1}{4}\sum_{i=1}^{4} |\Psi_i\rangle^{AB}|\Psi_i\rangle^{CD}\langle\Psi_i|^{AB}\langle\Psi_i| \\ &= \tfrac{1}{4}\sum_{i=1}^{4} |\Psi_i\rangle^{AC}|\Psi_i\rangle^{BD}\langle\Psi_i|^{AC}\langle\Psi_i| \\ &= \tfrac{1}{4}\sum_{i=1}^{4} |\Psi_i\rangle^{AD}|\Psi_i\rangle^{BC}\langle\Psi_i|^{AD}\langle\Psi_i|. \end{aligned} \tag{3.3.21}$$

Tests like standard entanglement swapping as such become superfluous since these schemes

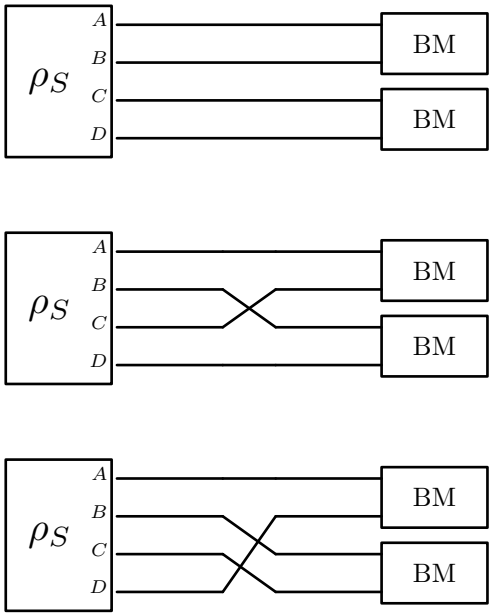

Figure 3.7: Three setups performing Bell measurement (BM) on the Smolin state ρ_S^{ABCD} to reveal party interchange symmetry.

represent a more general experiment.

CHAPTER 4

THE UNITARY INVARIANT STATES

Plus ça change, plus c'est la même chose.
- A. K.

The n-qubit singlet states $|\mathcal{S}_n^{(n)}\rangle$ are n-laterally unitary invariant[11], meaning that if an unitary operator U is applied to each qubit, the state remains the same, i.e.

$$U^{\otimes n}|\mathcal{S}_n^{(n)}\rangle = |\mathcal{S}_n^{(n)}\rangle. \tag{4.1}$$

This also implies that correlations between qubits remain the same for sets of measurements differing by an n-lateral unitary transformation. For example, when detecting $|\mathcal{S}_n^{(n)}\rangle$ in a photonic framework, an offset angle of the polarization analyzers will not effect the experiment outcome, as long as all analyzers have the same offset.
The n-qubit singlet states themselves are given by

$$|\mathcal{S}_n^{(2)}\rangle = \frac{1}{\frac{n}{2}!\sqrt{\frac{n}{2}+1}} \sum_{\forall\,(i,j,\ldots,m)\in P(0\ldots01\ldots1)} z!\left(\frac{n}{2}-z\right)!(-1)^{\frac{n}{2}-z}|ij\ldots m\rangle, \tag{4.2}$$

where n is even, $P(0\ldots01\ldots1)$ is the set of all possible permutations of $n/2$ zeros and $n/2$ ones and z is the number of zeros in the first $n/2$ positions. For $n = 2$ this is the familiar two-qubit singlet

$$|\mathcal{S}_2^{(2)}\rangle = |\Psi^-\rangle = \frac{1}{\sqrt{2}}\left(|01\rangle - |10\rangle\right). \tag{4.3}$$

For $n = 4$ we get

$$|\mathcal{S}_4^{(2)}\rangle = \frac{1}{2\sqrt{3}}\left(2|0011\rangle - |0101\rangle - |0110\rangle - |1001\rangle - |1010\rangle + 2|1100\rangle\right). \tag{4.4}$$

For brevity we will henceforth call the "n-laterally unitary invariant states" just "invariant states". (Phew!) The n-lateral unitary invariance draws to mind the stabilizer formalism as presented in [27] and briefly discussed in sections 2.4.5 and 3.3.3. Evidently, every n-lateral unitary operator acts as a stabilizing operator for these states. This is why finding a stabilizer entanglement witnesses for an invariant state seems to be feasible task. Below are presented three witnesses for the 4-qubit, 6-qubit and 8-qubit invariant states respectively.

4.1 Stabilizer-based witness for the 4-qubit invariant state

A maximum overlap witness for the 4-qubit invariant state is given in [16]:

$$\mathcal{W}_4 = \frac{3}{4}\mathbb{I}^{\otimes 4} - |\mathcal{S}_4^{(2)}\rangle\langle\mathcal{S}_4^{(2)}|. \tag{4.1.1}$$

The factor $\frac{3}{4}$ is the maximum overlap between $|\mathcal{S}_4^{(2)}\rangle$ and all product states. This witness was shown to be measurable in 15 measurement settings and it provides a noise tolerance of $p = \frac{4}{15} = 0.2667....$ The objective here will be to use the stabilizer framework to simplify this witness with respect to the number of measurements, while maintaining a high noise tolerance.

The simplest stabilizing operators for this state (4.4) are obviously the 4-lateral unitaries:

$$\mathcal{S}_1 = \sigma_x^{\otimes 4} \tag{4.1.2}$$
$$\mathcal{S}_2 = \sigma_y^{\otimes 4} \tag{4.1.3}$$
$$\mathcal{S}_3 = \sigma_z^{\otimes 4}. \tag{4.1.4}$$

These operators leave the (4.4) intact, but it was already known from section 3.3.3 that they only suffice to show that the state is not triseparable. Biseparability remains unproven. To remedy this, it is necessary to stray somewhat from the stabilizer formalism. Let's begin with the local decomposition of (4.4).

$$\rho_{\mathcal{S}_4} = \tag{4.1.5}$$
$$|\mathcal{S}_4^{(2)}\rangle\langle\mathcal{S}_4^{(2)}| = \tfrac{1}{16}\Big(\mathbb{IIII} + xxxx + yyyy + zzzz \tag{4.1.6}$$
$$+\frac{2}{3}\big(xyyx + yxxy + xyxy + yxyx\big) \tag{4.1.7}$$
$$+\frac{2}{3}\big(xzzx + zxxz + xzxz + zxzx\big) \tag{4.1.8}$$
$$+\frac{2}{3}\big(zyyz + yzzy + zyzy + yzyz\big) \tag{4.1.9}$$
$$+\frac{1}{3}\big(\mathbb{II}(xx + yy + zz) + (xx + yy + zz)\mathbb{II}\big) \tag{4.1.10}$$
$$-\frac{1}{3}\big(xx(yy + zz) + yy(xx + zz) + zz(xx + yy)\big) \tag{4.1.11}$$
$$-\frac{2}{3}\big(\mathbb{I}x\mathbb{I}x + \mathbb{I}xx\mathbb{I} + x\mathbb{I}x\mathbb{I} + x\mathbb{II}x\big) \tag{4.1.12}$$
$$-\frac{2}{3}\big(\mathbb{I}y\mathbb{I}y + \mathbb{I}yy\mathbb{I} + y\mathbb{I}y\mathbb{I} + y\mathbb{II}y\big) \tag{4.1.13}$$
$$-\frac{2}{3}\big(\mathbb{I}z\mathbb{I}z + \mathbb{I}zz\mathbb{I} + z\mathbb{I}z\mathbb{I} + z\mathbb{II}z\big)\Big) \tag{4.1.14}$$

Here, the tensor product $\otimes$ is implicit between each factor of every term and the Pauli matrices σ_x, σ_x and σ_x are denoted x, y and z respectively. The stabilizer terms (4.1.2) - (4.1.4) are visible on line (4.1.6). These terms together require 3 measurement settings, i.e. measuring the observables $xxxx$, $yyyy$ and $zzzz$. Trying to get the most out these settings, the terms on rows (4.1.10) and (4.1.12)-(4.1.14), containing only one variety of the Pauli

matrices along with the identity matrix, become interesting. However, when asserted as stabilizing operators, these terms fail. This can be seen by e.g.:

$$\begin{aligned}
\mathbb{I}\mathbb{I}xx|\mathcal{S}_4^{(2)}\rangle &= \mathbb{I}\mathbb{I}xx\frac{1}{2\sqrt{3}}\left(2|0011\rangle - |0101\rangle - |0110\rangle - |1001\rangle - |1010\rangle + 2|1100\rangle\right) \\
&= \frac{1}{2\sqrt{3}}\left(2|0000\rangle - |0110\rangle - |0101\rangle - |1010\rangle - |1001\rangle + 2|1111\rangle\right) \\
&\neq |\mathcal{S}_4^{(2)}\rangle
\end{aligned}$$

Apparently, $\mathbb{I}\mathbb{I}xx$ did transform the "inner" terms among themselves nicely, but destroyed the two remaining terms. This goes for every other similar combination of one type of Pauli matrix and the identity opertor. (From here on, such a combination will be called a Non-Mixed Pauli operator or NMP for short.) However, the sum of these terms *is* a stabilizing operator:

$$\begin{aligned}
\Theta_{NMP} = \tfrac{1}{6}\Big(& \frac{1}{3}\big(\mathbb{I}\mathbb{I}(xx+yy+zz) + (xx+yy+zz)\mathbb{I}\mathbb{I}\big) && (4.1.15)\\
& -\frac{2}{3}\big(\mathbb{I}x\mathbb{I}x + \mathbb{I}xx\mathbb{I} + x\mathbb{I}x\mathbb{I} + x\mathbb{I}\mathbb{I}x\big) && (4.1.16)\\
& -\frac{2}{3}\big(\mathbb{I}y\mathbb{I}y + \mathbb{I}yy\mathbb{I} + y\mathbb{I}y\mathbb{I} + y\mathbb{I}\mathbb{I}y\big) && (4.1.17)\\
& -\frac{2}{3}\big(\mathbb{I}z\mathbb{I}z + \mathbb{I}zz\mathbb{I} + z\mathbb{I}z\mathbb{I} + z\mathbb{I}\mathbb{I}z\big)\Big). && (4.1.18)
\end{aligned}$$

Note that the original terms have been multiplied by $\frac{8}{3}$ to give obtain a correct normalization when Θ_{NMP} is applied to the invariant state:

$$\Theta_{NMP}|\mathcal{S}_4^{(2)}\rangle = |\mathcal{S}_4^{(2)}\rangle, \tag{4.1.19}$$

which proves that Θ_{NMP} is indeed a stabilizing operator. It may be possible that some subsets of these terms also stabilizes $|\mathcal{S}_4^{(2)}\rangle$.

Following the subsequent steps of the stabilizer witness programme (e.g. calculating overlaps) yields a witness detecting the $|\mathcal{S}_4^{(2)}\rangle$, but which has a poor noise tolerance. The stabilizer framework is jettisoned here, since it was found that a much better witness was produced by leaving the coefficients for the stabilizing terms intact as they stand in the local decomposition (4.1.6)-(4.1.14). This witness is described below.

4.1.1 Reduced witness for the 4-qubit invariant state

Extracting the NMP's along with the 4-lateral Pauli operators from the local decomposition, gives a *reduced witness*:

$$\begin{aligned}
\mathcal{W}_4' = \; & c_0\mathbb{I}\mathbb{I}\mathbb{I}\mathbb{I} - \frac{1}{16}\Big(xxxx + yyyy + zzzz \\
& + \frac{1}{3}\big(\mathbb{I}\mathbb{I}(xx+yy+zz) + (xx+yy+zz)\mathbb{I}\mathbb{I}\big) \\
& - \frac{2}{3}\big(\mathbb{I}x\mathbb{I}x + \mathbb{I}xx\mathbb{I} + x\mathbb{I}x\mathbb{I} + x\mathbb{I}\mathbb{I}x\big) \\
& - \frac{2}{3}\big(\mathbb{I}y\mathbb{I}y + \mathbb{I}yy\mathbb{I} + y\mathbb{I}y\mathbb{I} + y\mathbb{I}\mathbb{I}y\big) \\
& - \frac{2}{3}\big(\mathbb{I}z\mathbb{I}z + \mathbb{I}zz\mathbb{I} + z\mathbb{I}z\mathbb{I} + z\mathbb{I}\mathbb{I}z\big)\Big). && (4.1.20)
\end{aligned}$$

The value of the constant c_0 is dictated by the equation

$$\mathcal{W}_4' \geq \alpha \mathcal{W}_4, \text{ for some } \alpha > 0, \tag{4.1.21}$$

which restricts $\mathcal{W}_4'$ to detecting fewer inseparable states than the maximum overlap witness $\mathcal{W}_4$, thus ensuring that the resulting witness will detect true multi-qubit entanglement, if any entanglement at all. Within the bounds of (4.1.21), c_0 ought to be minized to allow for greater noise tolerance. The function

$$\min(\text{eig}(\mathcal{W}_4')_{\,|\,c_0=0} - \alpha \min(\text{eig}(\mathcal{W}_4')) \tag{4.1.22}$$

has exactly one global maximum which occurs for $\alpha = \frac{5}{12}$, giving a minimum c_0 of $\frac{11}{24}$. Using this value for c_0 gives a witness with a noise tolerance of $p = \frac{5}{27} = 0.1802...$, not far from the noise tolerance $p = 0.2667...$ of the maximum overlap witness.

4.2 Generalizations of the 4-qubit reduced witness

The reduced witness $\mathcal{W}_4'$ above can be expressed

$$\mathcal{W}_4' = c_0^{(4)} \mathbb{IIII} - \frac{1}{16} \sum_{p \in P_4} \text{tr}(p \rho_{\mathcal{S}_4}) p, \tag{4.2.1}$$

where P_4 is the set of all unique permutations of all 4-qubit-NMP's with an even, non-zero, number of Pauli operators, including the 4-lateral operators of (4.1.2)-(4.1.4). This is exactly the terms of (4.1.20). The constant $c_0^{(4)}$ is derived from comparison with the maximum overlap witness, as above. It is now easy to see that this recipe can be expanded to higher dimensions. The n-dimensional witness candidate is:

$$\mathcal{W}_n = c_0^{(n)} \mathbb{I}^{\otimes n} - \frac{1}{2^n} \sum_{p \in P_n} \text{tr}(p \rho_{\mathcal{S}_n}) p, \quad n \text{ even}, \tag{4.2.2}$$

where P_n is the set of all unique permutations of all n-qubit-NMP's with an even, non-zero, number of Pauli operators, including the n-lateral operators $\sigma_x^{\otimes n}$, $\sigma_y^{\otimes n}$ and $\sigma_z^{\otimes n}$. In analogy with the 4-dimensional case, the constant is derived from

$$\mathcal{W}_n' \geq \alpha \mathcal{W}_n, \text{ for some } \alpha > 0, \tag{4.2.3}$$

where $\mathcal{W}_n$ is the maximum overlap witness.

4.2.1 Reduced witness for the 6-qubit invariant state

The approach above works fine for $n = 6$, where the witness has $c_0^{(6)} = 0.3142...$ and a noise tolerance $p = 0.1502....$ The maximum overlap witness for $n = 6$ has a noise tolerance of $p = 0.3386...$, so the reduced witness is about half that. However, the reduced witness is still measurable in three settings while the maximum overlap witness with its 544 terms would require on the order of hundreds of measurements[1].

[1] Usually, some rearrangements can be made, allowing measurement several terms in one setting.

4.2.2 Reduced witness for the 8-qubit invariant state

For $n = 8$, the reduced witness has $c_0^{(8)} = 0.2281...$ and $p = 0.0751....$ The noise tolerances for the maximum overlap witness for $n = 8$ is $p = 0.3765....$ Again, since the maximum overlap witness has so many terms, 8320 to be exact, the reduced three setting witness $\mathcal{W}_8'$ might prove useful in spite of its rather low noise tolerance.

4.2.3 Venturing further

When testing the witness candidate for $n = 10$, with $c_0^{(10)} = 0.1778...$, a noise tolerance of $p = 0$ was found. Consequently, the witness candidate was discarded as invalid. Obviously, the "cross-Pauli" terms, such as (4.1.7)-(4.1.9), make up a larger and larger portion of the invariant states as dimensionality increases, reducing the importance of the NMP's, thus decreasing the noise tolerance. In order for a reduced witness of higher dimensionality to be useful, it must incorporate additional "cross-Pauli" terms. It is possible that there is a simple scheme for attaining these witnesses, but that is well beyond the scope of this report.

The calculations the reduced witnesses were performed in MATLAB with the program-files are shown in Appendix B.

CHAPTER 5

CONCLUSION AND OUTLOOK

The future is here. It's just not widely distributed yet.
- W. G.

5.1 The Smolin state

This report set out to show a realistic way of creating a bound entangled state in experiment. The Smolin state became the obvious candidate due to its remarkable properties, which not only grant it a special place among the bound entangled states, but also reduce the resources needed to produce and analyze it. Four experimental setups that produce the Smolin state were presented. Three of these were based on standard quantum gates, differing in their initial conditions and using 10, 6 and 6 gates, respectively. Now, in 2009, constructing quantum gates is still a hard task, which is why a fourth setup was pursued. Working only with single-qubit operations and a two-photon entanglement source, this setup demonstrates a way of creating bound entanglement which is already well within reach today.

With an experiment already producing the Smolin state, one has the task of examining its entanglement content. For this purpose an entanglement witness was derived. This witness was measurable in only three measurement settings, a feature stemming from the unique symmetry properties of the state. The noise tolerance for this witness was $p = \frac{2}{3}$, which is maximal, since above this limit the Smolin state ceases to be entangled. It was subsequently shown that this derived maximum overlap witness coincided with a witness produced by means of the stabilizer formalism. The latter approach also gave another, simplified witness measurable in a minimal two settings, while providing a noise tolerance $p = \frac{1}{2}$.

Finally, means to discriminate the Smolin state from other Bell state combinations and an experimental setup for examining the symmetry properties of the state were given.

The setups and tools above are suggestions for a real experiment yet to be performed. Some of the theoretic groundwork has thus been laid, while other aspects have not been elaborated upon. One of these is the calculational task involved in setting up and tuning a photonic system, which would have to be undertaken when an experiment is within grasp. It seems highly probable that when the Smolin state is produced this would be in a photonic framework, since other systems would be hard pressed to reach the sufficient number of qubits and/or complexity of the operations performable on these.

Regardless of the manner in which the Smolin state is produced, its production would provide insight into exotic phenomena around quantum entanglement, such as bound entanglement, unlockability and the effects of bipartite entanglement combined with party interchange symmetry. Apart from these aspects, the Smolin state can be put to use in quantum computation with e.g. quantum secret sharing and remote information concentration.
As a final note on the Smolin state, it is fitting to mention that recently, Wang and Ying[37] showed that stabilizers may be employed to produce families of bound entangled *and* unlockable states, including the Smolin state and its generalizations[36]. Not only do these contructions reproduce the Smolin state in a very simple manner, but they explain all of its properties with magnificent clarity.

5.2 The invariant states

While this report was dedicated to the generation of the Smolin from early on, a second parallel theme soon appeared, concerning the n-lateral unitary invariant states. These states had been shown to withstand noise well and were already used in experiments in the case of $n = 4$. However, as for most 4-qubit states, the maximum overlap entanglement witness used to verify its entanglement content required many measurement settings, in this case 15. A way was sought to reduce the complexity and the number of measurements of the witness and its higher dimensional counterparts.

Starting by using the stabilizer framework and continuing by extracting terms from the local decomposition of the 4-qubit invariant state, a witness was produced which was measurable in three settings and provided a noise tolerance of $p = \frac{5}{27} = 0.1802...$ to be compared to that of the original 15 setting witness at $p = 0.2667....$ The witness detects genuine multipartite entanglement. The procedure used for this witness proved to be adaptable to higher dimensional invariant states, generating three setting witnesses for the 6-qubit and 8-qubit witnesses with noise tolerances of $p = 0.1502...$ and $p = 0.0751...$, respectively. Although the corresponding maximum overlap witnesses have noise tolerances around $p = \frac{1}{3}$, they require a number of measurements on the orders of 100's, and in the case of 8-qubits, 1000's, of measurements, thus justifying their replacement by a three setting witness with a low noise tolerance.

When trying to move beyond 8 qubits, the three setting approach of the witnesses above did not suffice. In these higher dimensional cases, the witnesses presented in this thesis still provide a good basis in the search for a simplified witness where additional terms of the local decomposition of the particular invariant state are taken into account.

APPENDIX A

CALCULATIONS FOR GENERATION OF THE SMOLIN STATE

A.1 Calculation of the yield of the first setup

Below are the calculations for the state produced by setup 1 as described on page 29 and presented in fig. 3.3.

Stage 1, Preparation: The preparation stage sets up the ancillae and produces a 4-party standard GHZ state.

$$\begin{aligned}
&|0\rangle^A|0\rangle^B|0\rangle^C|0\rangle^D|0\rangle^E|0\rangle^F \equiv |000000\rangle \quad \overset{H_A, H_E, H_F}{\Longrightarrow} \\
&\tfrac{1}{2\sqrt{2}}\left(|0\rangle+|1\rangle\right)|000\rangle\left(|0\rangle+|1\rangle\right)\left(|0\rangle+|1\rangle\right) \quad \overset{CNOT_{AB}, CNOT_{AC}, CNOT_{AD}}{\Longrightarrow} \\
&\tfrac{1}{2\sqrt{2}}\left(|0000\rangle+|1111\rangle\right)\left(|00\rangle+|01\rangle+|10\rangle+|11\rangle\right)
\end{aligned} \tag{A.1.1}$$

Stage 2, Modification: The second stage modifies the qubits of the produced GHZ state and couples these to the ancillae.

$$\begin{aligned}
&\tfrac{1}{2\sqrt{2}}\left(|0000\rangle+|1111\rangle\right)\left(|00\rangle+|01\rangle+|10\rangle+|11\rangle\right) \quad \overset{CNOT_{EA}, CNOT_{FB}}{\Longrightarrow} \\
&\tfrac{1}{2\sqrt{2}}\big(\left(|0000\rangle+|1111\rangle\right)|00\rangle+\left(|0100\rangle+|1011\rangle\right)|01\rangle+ \\
&\qquad\left(|1000\rangle+|0111\rangle\right)|10\rangle+\left(|1100\rangle+|0011\rangle\right)|11\rangle\big) \quad \overset{CNOT_{EC}, CNOT_{FC}}{\Longrightarrow} \\
&|\Psi_S\rangle^{ABCDEF} = \tfrac{1}{2\sqrt{2}}\big(\left(|0000\rangle+|1111\rangle\right)|00\rangle+\left(|0110\rangle+|1001\rangle\right)|01\rangle \\
&\qquad\qquad +\left(|1010\rangle+|0101\rangle\right)|10\rangle+\left(|1100\rangle+|0011\rangle\right)|11\rangle\big) \\
&= \tfrac{1}{2}\big(|\Psi_1^{GHZ}\rangle|00\rangle+|\Psi_4^{GHZ}\rangle|01\rangle+|\Psi_3^{GHZ}\rangle|10\rangle+|\Psi_2^{GHZ}\rangle|11\rangle\big)
\end{aligned} \tag{A.1.2}$$

Stage 3, Trace: Finally, from the state $|\Psi_S\rangle$ we get,

$$\mathrm{Tr}_{E,F}|\Psi_S\rangle^{ABCDEF}\langle\Psi_S| = \frac{1}{4}\sum_{i=1}^{4}|\Psi_i^{GHZ}\rangle^{ABCD}\langle\Psi_i^{GHZ}| = \rho_S^{ABCD}. \tag{A.1.3}$$

A.2 Calculation of the yield of the second setup

Since stage 1 of setup 1 produces a GHZ state, the calculation of the yield of setup 2 is simply stage 2 and 3 along with the preparation of the ancillae of setup 1 in the section above.

A.3 Calculation of the yield of the third setup

Below are the calculations for the state produced by setup 3 as described on page 30 and presented in fig. 3.5. To simplify matters, the initial EPR-pair is chosen to $\Psi_i = \Psi_4 = \Phi^+$, it is however clear that the result will be the same regardless of which Ψ_i s used.

$$|\Phi^+\rangle^{AB}|\Phi^+\rangle^{CD}|00\rangle^{EF} = \tfrac{1}{2}(|00\rangle + |11\rangle)(|00\rangle + |11\rangle)|00\rangle \quad \overset{H_E, H_F}{\Longrightarrow}$$

$$\tfrac{1}{4}(|00\rangle + |11\rangle)(|00\rangle + |11\rangle)(|0\rangle + |1\rangle)(|0\rangle + |1\rangle) \quad \overset{CNOT_{EB}, CNOT_{ED}}{\Longrightarrow}$$

$$\tfrac{1}{4}\left((|00\rangle + |11\rangle)(|00\rangle + |11\rangle)|0\rangle + (|01\rangle + |10\rangle)(|01\rangle + |10\rangle)|1\rangle(|0\rangle + |1\rangle)\right) \quad \overset{P_{FA}, P_{FC}}{\Longrightarrow}$$

$$\begin{aligned}|\Phi_S\rangle^{ABCDEF} =& \tfrac{1}{4}((|00\rangle + |11\rangle)(|00\rangle + |11\rangle)|00\rangle + (|00\rangle - |11\rangle)(|00\rangle - |11\rangle)|01\rangle \\ &+(|01\rangle + |10\rangle)(|01\rangle + |10\rangle)|10\rangle + (|01\rangle - |10\rangle)(|01\rangle - |10\rangle)|11\rangle) \\ =& \tfrac{1}{2}(|\Phi^+\rangle|\Phi^+\rangle|00\rangle + |\Phi^-\rangle|\Phi^-\rangle|01\rangle + |\Psi^+\rangle|\Psi^+\rangle|10\rangle + |\Psi^-\rangle|\Psi^-\rangle|11\rangle)\end{aligned}$$

Once $|\Phi_S^{ABCDEF}\rangle$ is obtained, the Smolin state is produced by the trace:

$$\mathrm{Tr}_{E,F}|\Phi_S\rangle^{ABCDEF}\langle\Phi_S| = \frac{1}{4}\sum_{i=1}^{4}|\Psi_i\rangle|\Psi_i\rangle^{ABCD}\langle\Psi_i|\langle\Psi_i| = \rho_S^{ABCD} \tag{A.3.1}$$

A.4 Calculation of the yield of the fourth setup

Below are the calculations for the state produced by setup 4 as described on page 31 and presented in fig. 3.6. The strategy of setup 4 is similar to that of setup 3 but differing in that no ancillae are used to provide the mixing, since a six-photon system may be too taxing to set up.
A single photon passing the BBO results in the following state

$$O_1 = \frac{1}{\sqrt{2}}(a_{1v}^\dagger a_{2h}^\dagger + a_{1h}^\dagger a_{2v}^\dagger), \tag{A.4.1}$$

which passes HWP2,

$$\begin{aligned}O_1 \quad \overset{HWP2}{\Longrightarrow} \quad O_2 =& \tfrac{1}{\sqrt{2}}\Big(\big((\cos^2\phi - \sin^2\phi)a_{1v}^\dagger + (\sin 2\phi)a_{1h}^\dagger\big)a_{2h}^\dagger \\ &+\big((\sin 2\phi)a_{1v}^\dagger + (\sin^2\phi - \cos^2\phi)a_{1h}^\dagger\big)a_{2v}^\dagger\Big)\end{aligned} \tag{A.4.2}$$

We will only be interested in $\phi = \phi_1 = 0$ and $\phi = \phi_2 = \frac{\pi}{2}$ for which we can conveniently write

$$\begin{aligned} O_3 = O_2 \,\big|\, _{\phi\in\{\phi_1=0,\,\phi_2=\frac{\pi}{2}\}} = &\tfrac{1}{\sqrt{2}}\big((\delta_{\phi\phi_1}a^\dagger_{1v} + \delta_{\phi\phi_2}a^\dagger_{1h})a^\dagger_{2h} \\ &+(\delta_{\phi\phi_2}a^\dagger_{1v} - \delta_{\phi\phi_1}a^\dagger_{1h})a^\dagger_{2v}\big) \end{aligned} \tag{A.4.3}$$

Taking into account QWP1

$$\begin{aligned} &O_3 \quad \overset{QWP1}{\Longrightarrow} \\ &O_4 = \tfrac{1}{\sqrt{2}}\big((\delta_{\phi\phi_1}a^\dagger_{1v} + \delta_{\phi\phi_2}a^\dagger_{1h})e^{\frac{-2\pi ci}{\cos\theta}}a^\dagger_{2h} + (\delta_{\phi\phi_2}a^\dagger_{1v} - \delta_{\phi\phi_1}a^\dagger_{1h})a^\dagger_{2v}\big) \end{aligned} \tag{A.4.4}$$

It is only the values of θ where $e^{\frac{2\pi ci}{\cos\theta}} = \pm 1$ that we will concern ourselves with. These occur at

$$\theta^+ = \arccos\left(\frac{2c}{1+2n}\right),\ n \in \mathbb{Z}_+ \tag{A.4.5}$$

$$\theta^- = \arccos\left(\frac{c}{n}\right),\ n \in \mathbb{Z}_+ \setminus 0. \tag{A.4.6}$$

Again for convenience,

$$\begin{aligned} O_5 = O_4 \,\big|\, _{\theta\in\{\theta^+,\,\theta^-\}} = &\tfrac{1}{\sqrt{2}}\big((\delta_{\theta\theta^+} - \delta_{\theta\theta^-})(\delta_{\phi\phi_1}a^\dagger_{1v} + \delta_{\phi\phi_2}a^\dagger_{1h})a^\dagger_{2h} \\ &+(\delta_{\phi\phi_2}a^\dagger_{1v} - \delta_{\phi\phi_1}a^\dagger_{1h})a^\dagger_{2v}\big) \end{aligned} \tag{A.4.7}$$

Passing the beam splitters BS1 and BS2 gives

$$\begin{aligned} &O_5 \quad \overset{BS1,BS2}{\Longrightarrow} \\ &O_6 = \tfrac{1}{2\sqrt{2}}\big((\delta_{\theta\theta^+} - \delta_{\theta\theta^-})(\delta_{\phi\phi_1}(a^\dagger_{Av} + ia^\dagger_{Bv}) + \delta_{\phi\phi_2}(a^\dagger_{Ah} + ia^\dagger_{Bh}))(a^\dagger_{Ch} + ia^\dagger_{Dh}) \\ &\quad +(\delta_{\phi\phi_2}(a^\dagger_{Av} + ia^\dagger_{Bv}) - \delta_{\phi\phi_1}(a^\dagger_{Ah} + ia^\dagger_{Bh}))(a^\dagger_{Cv} + ia^\dagger_{Dv})\big) \end{aligned} \tag{A.4.8}$$

To proceed we must take into account that the laser used in this setup is pulsed. Photons belonging to different laser pulses can be thought of as existing in different temporal modes. This will reflect in annihilation (creation) operators by the appending of a third quantum number. These will consequently follow the convention, $a^{(\dagger)}_{spt}$, where s, p and t are spatial, polarization and temporal modes respectively. As an example, $a^\dagger_{1v2}$ represents a vertically polarized photon in spatial mode 1 and temporal mode 2. In analogy to the spatial modes, the temporal modes are orthogonal.
Keeping θ and ϕ constant between pulses, O_6 becomes

$$\begin{aligned} O_6(t) = &\tfrac{1}{2\sqrt{2}}\big((\delta_{\theta\theta^+} - \delta_{\theta\theta^-})(\delta_{\phi\phi_1}(a^\dagger_{Avt} + ia^\dagger_{Bvt}) + \delta_{\phi\phi_2}(a^\dagger_{Aht} + ia^\dagger_{Bht}))(a^\dagger_{Cht} + ia^\dagger_{Dht}) \\ &+(\delta_{\phi\phi_2}(a^\dagger_{Avt} + ia^\dagger_{Bvt}) - \delta_{\phi\phi_1}(a^\dagger_{Aht} + ia^\dagger_{Bht}))(a^\dagger_{Cvt} + ia^\dagger_{Dvt})\big). \end{aligned} \tag{A.4.9}$$

Looking at the combined state from two consequtive pulses in temporal modes $t = 1$ and

$t = 2$ passing through the delay lines DL1 and DL2

$$O_6(1) \otimes O_6(2) \quad \overset{DL1,DL2}{\Longrightarrow}$$

$$\begin{aligned} O_7 =& \tfrac{1}{2\sqrt{2}}\big((\delta_{\theta\theta^+} - \delta_{\theta\theta^-})(\delta_{\phi\phi_1}(a^\dagger_{Av1} + ia^\dagger_{Bv2}) + \delta_{\phi\phi_2}(a^\dagger_{Ah1} + ia^\dagger_{Bh2}))(a^\dagger_{Ch1} + ia^\dagger_{Dh2}) \\ &+(\delta_{\phi\phi_2}(a^\dagger_{Av1} + ia^\dagger_{Bv2}) - \delta_{\phi\phi_1}(a^\dagger_{Ah1} + ia^\dagger_{Bh2}))(a^\dagger_{Cv1} + ia^\dagger_{Dv2})\big) \\ \otimes& \tfrac{1}{2\sqrt{2}}\big((\delta_{\theta\theta^+} - \delta_{\theta\theta^-})(\delta_{\phi\phi_1}(a^\dagger_{Av2} + ia^\dagger_{Bv3}) + \delta_{\phi\phi_2}(a^\dagger_{Ah2} + ia^\dagger_{Bh3}))(a^\dagger_{Ch2} + ia^\dagger_{Dh3}) \\ &+(\delta_{\phi\phi_2}(a^\dagger_{Av2} + ia^\dagger_{Bv3}) - \delta_{\phi\phi_1}(a^\dagger_{Ah2} + ia^\dagger_{Bh3}))(a^\dagger_{Cv2} + ia^\dagger_{Dv3})\big) \end{aligned} \tag{A.4.10}$$

Post-selecting O_7, keeping only the case where four photons are present at the detectors PA1-PA4, which happens when all photons are in temporal mode $t = 2$, results in

$$\begin{aligned} O_8(\theta,\, \phi) = -\tfrac{1}{8}\big((\delta_{\theta\theta^+} - \delta_{\theta\theta^-})(\delta_{\phi\phi_1}a^\dagger_{Bv} + \delta_{\phi\phi_2}a^\dagger_{Bh})a^\dagger_{Dh} + (\delta_{\phi\phi_2}a^\dagger_{Bv} - \delta_{\phi\phi_1}a^\dagger_{Bh})a^\dagger_{Dv}\big) \\ \otimes\big((\delta_{\theta\theta^+} - \delta_{\theta\theta^-})(\delta_{\phi\phi_1}a^\dagger_{Av} + \delta_{\phi\phi_2}a^\dagger_{Ah})a^\dagger_{Ch} + (\delta_{\phi\phi_2}a^\dagger_{Av} - \delta_{\phi\phi_1}a^\dagger_{Ah})a^\dagger_{Cv}\big). \end{aligned} \tag{A.4.11}$$

Evaluating O_8 at the different combinations of θ and ϕ gives the following four outcomes

$$O_8(\theta^-,\, \phi_1) = -\frac{1}{8}\big(a^\dagger_{Bv}a^\dagger_{Dh} + a^\dagger_{Bh}a^\dagger_{Dv}\big) \otimes \big(a^\dagger_{Av}a^\dagger_{Ch} + a^\dagger_{Ah}a^\dagger_{Cv}\big) \tag{A.4.12}$$

$$O_8(\theta^-,\, \phi_2) = -\frac{1}{8}\big(a^\dagger_{Bh}a^\dagger_{Dh} - a^\dagger_{Bv}a^\dagger_{Dv}\big) \otimes \big(a^\dagger_{Ah}a^\dagger_{Ch} - a^\dagger_{Av}a^\dagger_{Cv}\big) \tag{A.4.13}$$

$$O_8(\theta^+,\, \phi_1) = -\frac{1}{8}\big(a^\dagger_{Bv}a^\dagger_{Dh} - a^\dagger_{Bh}a^\dagger_{Dv}\big) \otimes \big(a^\dagger_{Av}a^\dagger_{Ch} - a^\dagger_{Ah}a^\dagger_{Cv}\big) \tag{A.4.14}$$

$$O_8(\theta^+,\, \phi_2) = -\frac{1}{8}\big(a^\dagger_{Bh}a^\dagger_{Dh} + a^\dagger_{Bv}a^\dagger_{Dv}\big) \otimes \big(a^\dagger_{Ah}a^\dagger_{Ch} + a^\dagger_{Av}a^\dagger_{Cv}\big) \tag{A.4.15}$$

Letting these operators act on the photon number ground state $|0\rangle \equiv |0000\rangle^{BDAC}$,

$$O_8(\theta^-,\, \phi_1)|0\rangle = -\frac{1}{8}\big(|vh\rangle + |hv\rangle\big)^{\otimes 2} = -\frac{1}{4}|\Psi^+\rangle \otimes |\Psi^+\rangle \tag{A.4.16}$$

$$O_8(\theta^-,\, \phi_2)|0\rangle = -\frac{1}{8}\big(|hh\rangle - |vv\rangle\big)^{\otimes 2} = -\frac{1}{4}|\Phi^-\rangle \otimes |\Phi^-\rangle \tag{A.4.17}$$

$$O_8(\theta^+,\, \phi_1)|0\rangle = -\frac{1}{8}\big(|vh\rangle - |hv\rangle\big)^{\otimes 2} = -\frac{1}{4}|\Psi^-\rangle \otimes |\Psi^-\rangle \tag{A.4.18}$$

$$O_8(\theta^+,\, \phi_2)|0\rangle = -\frac{1}{8}\big(|hh\rangle + |vv\rangle\big)^{\otimes 2} = -\frac{1}{4}|\Phi^+\rangle \otimes |\Phi^+\rangle, \tag{A.4.19}$$

gives the Bell states up to a common constant.
By randomly selecting a $\theta \in \{\theta^-, \theta^+\}$ and a $\phi \in \{\phi_1, \phi_2\}$ after each recorded four-fold coincidence at the detectors, the full Smolin state is produced.

$$\sum_{\theta=\theta^-,\theta^+} \frac{1}{2} \sum_{\phi=\phi_1,\phi_2} \frac{1}{2}\big(O_8(\theta,\, \phi)|0\rangle\big)\big(\langle 0|O_8^\dagger(\theta,\, \phi)\big) = \frac{1}{16}\sum_{i=1}^{4}\frac{1}{4}|\Psi_i\rangle \otimes |\Psi_i\rangle\langle\Psi_i| \otimes \langle\Psi_i| \propto \rho_S^{ABCD}, \tag{A.4.20}$$

as required. The factor $\frac{1}{16}$ is the portion of the initially produced EPR pairs that gives rise to fourfold coincidences.

APPENDIX B

CALCULATIONS FOR REDUCED WITNESSES FOR THE 4-, 6-, 8- AND 10-QUBIT INVARIANT STATES

Below are presented the MATLAB files used to calculate the reduced witnesses of chapter 4.

B.1 Witnesses_for_the_Invariant_States_01.m

```
%%Filename: Witnesses_for_the_Invariant_States_01.m
clear all
for dim=[4:2:10]
    '======================================'
    tic;
    dim
    %%The Invariant State of dimension dim
    invariant_state=invariant(dim);
    invariant_state=invariant_state*invariant_state';

    %%Constructing the projector witness
    'Projector witness'
    max_overlap_non_permuted=overlap(invariant_state)
    max_overlap=max_subset_overlap(invariant_state)
    projector_witness=max_overlap*eye(2^dim)-invariant_state;
    noise_tolerance_projector=...
      noise_tolerance(projector_witness, invariant_state)

    %%Constructing the reduced witness
    'Reduced witness'
    reduced_witness=pauli_trace_out(invariant_state);
```

```
    alpha=maximum(-reduced_witness, projector_witness, [0,1], 6);
    c0=min(eig(alpha*projector_witness))-min(eig(-reduced_witness))
    t=max_subset_overlap(reduced_witness);
    if t>c0
        'Not a viable witness, does not discriminate biseparable states.'
        return;
    end;
    reduced_witness=c0*eye(2^dim)-reduced_witness;
    min_eig=min(eig(reduced_witness))
    reduced_witness_on_invariant_state=trace(reduced_witness*invariant_state)
    noise_tolerance_reduced=noise_tolerance(reduced_witness, invariant_state)

    save(['variables for the ', num2str(dim), '-qubit invariant state']);
    time_for_calculation=toc
end;
return;
```

B.2 invariant.m

```
%%Filename: invariant.m
%Constructs an invariant state of dimension n
function sum_n2=invariant(n)
v=[zeros(1,n/2),ones(1,n/2)];
%All permutations
p=perms(v);
%Corrected permutations
np=zeros(1,n);
psize=size(p);
for i=1:psize(1)
    flag=0;
    npsize=size(np);
    for j=1:npsize(1)
        if(np(j,:)==p(i,:))
            flag=1;
        end %if
    end %for
    if(flag==0)
        np(npsize(1)+1,:)=p(i,:);
    end %if
end %for
npsize=size(np);
np=np(2:npsize(1),:);

%Construct the helper vector
helper=1/2*cumprod(2*ones(1,n));
%Parser
```

```
parts=np*helper';
no_of_z=n/2-sum(np(:, 1:n/2),2);
id_n=eye(2^n);
parts=id_n(parts+1, :);
sum_n2=0;
zsize=size(no_of_z);
for i=1:zsize(1)
    sum_n2=sum_n2+factorial(no_of_z(i))...
    *factorial(n/2-no_of_z(i))*(-1)^(n/2-no_of_z(i))*parts(i,:);
end %for
sum_n2=sum_n2'/(factorial(n/2)*sqrt(n/2+1));
```

B.3 overlap.m

```
%%Filename: overlap.m
%Returns the maximum overlap between all bipartite states and rho.
function max_eig=overlap(rho)
n=log2(length(rho));
parts=cumsum(ones(1,n));
max_eig=-Inf;
for i=1:(n-1)
    div=nchoosek(parts,i);
    divsize=size(div);
    for j=1:divsize(2)
        max_eig_temp=max(eig(keep(rho, div(j,:))));
        if(max_eig_temp>max_eig)
            max_eig=max_eig_temp;
        end
    end
end
```

B.4 max_subset_overlap.m

```
%%Filename: max_subset_overlap.m
%Finds the overlap between state and symmetrized
%biseparable states based on invariant states.
function max_overlap=max_subset_overlap(state)
    dim=log2(length(state));
    biseparables=construct_biseparables(dim);
    max_overlap=-Inf;
    for i=[1:length(biseparables)]
        max_overlap=max(trace(biseparables{i}*state), max_overlap);
    end;
```

B.5 construct_biseparables.m

```
%%Filename: construct_biseparables.m
%Calculates all the possible symmetrized
%biseparable states based on invariant states.
function res=construct_biseparables(dim)
order=[dim:-1:1];
counter=1;
res={};
for i=[2:2:dim/2]
    inv1=invariant(dim-i);
    inv2=invariant(i);
    inv1=inv1*inv1';
    inv2=inv2*inv2';

    center=right_shift_vector(order, (dim-i)/2);
    res{counter}=reorder(mkron(inv1, inv2), center);
    counter=counter+1;
end;
```

B.6 noise_tolerance.m

```
%%Filename: noise_tolerance.m
%Calculates the noise tolerance of an entanglement witness
%for a particular state.
function p=noise_tolerance(witness, state)
p=-trace(witness*state)/(trace(witness)/length(witness)-trace(witness*state));
```

B.7 pauli_trace_out.m

```
%%Filename: pauli_trace_out.m
%Returns all the Non-Mixed Pauli operators and n-lateral
%Pauli ops for the given state. It is assumed that the
%state has the same for x, y and z NMPs.
function res=pauli_trace_out(state)
I=sqrt(-1);
x=[0,1;1,0];
y=[0,-I;I,0];
z=[1,0;0,-1];
p={x,y,z};


qubits=log2(length(state));
res=zeros(length(state));
for i=[1:length(state)-1]
    c=bin(i,qubits);
    if(mod(num_set_bits(c),2)==0)
```

```
        ci=bin_invert(c);
        p_opx=c(1)*x+ci(1)*eye(2);
        p_opy=c(1)*y+ci(1)*eye(2);
        p_opz=c(1)*z+ci(1)*eye(2);
        for j=[2:qubits]
            p_opx=mkron(p_opx, c(j)*x+ci(j)*eye(2));
            p_opy=mkron(p_opy, c(j)*y+ci(j)*eye(2));
            p_opz=mkron(p_opz, c(j)*z+ci(j)*eye(2));
        end;
        t=trace(state*p_opx)/length(state);

        res=res+t*p_opx;
        res=res+t*p_opy;
        res=res+t*p_opz;
    end;
end;
```

B.8 maximum.m

```
%%Filename: maximum.m
%A (very) simple method for finding the alpha at the maximum of
%eig(test_witness-alpha*projector_witness) for a given
%interval of alpha.
function res=maximum(test_witness,projector_witness, alpha_interval, level)
max_value=-Inf;
max_alpha=-Inf;
no_of_intervals=100;
for alpha=linspace(alpha_interval(1),alpha_interval(2),no_of_intervals)
    eigs=eig(test_witness-alpha*projector_witness);
    if eigs(1)>max_value
        max_value=eigs(1);
        max_alpha=alpha;
    end
end;

level=level-1;
if level>0
    half_interval=1.0*(alpha_interval(2)-alpha_interval(1))/no_of_intervals;
    res=maximum(test_witness, projector_witness,...
     [max_alpha-half_interval,max_alpha+half_interval], level);
else
    res=max_alpha;
end
```

BIBLIOGRAPHY

[1] Coined by Einstein as "spukhafte Fernwirkung", see e.g. M. Born, *Albert Einstein und das Lichtquantum*, Die Naturwissenschaften, Heft 15, Jg. 42, p. 430 (1955)

[2] B. d'Espagnat, *Conceptual Foundations of Quantum Mechanics*, Second Edition, p. 75 and p. 94, W. A. Benjamin (1976), Reading MA, USA

[3] E. Schrödinger, *Die gegenwärtige Situation in der Quantenmechanik*, Naturwissenschaften 23 #48, (Nov 1935)

[4] A. Einstein et al., *Can Quantum-Mechanical Description of Physical Reality Be Considered Complete?*, Phys. Rev. 47, pages 777 - 780, (1935)

[5] J. S. Bell, *On the Einstein Podolsky Rosen Paradox*, Physics 1 #3, pages 195 - 200, (1964)

[6] A. Aspect et al. *Experimental test of Bell's inequalities using time-varying analyzers*, Phys. Rev. Lett. 49 #25, 1804, (20 Dec 1982)

[7] R. P. Feynman, *Simulating Physics with Computers*, (1982)

[8] D. Deutsch, R. Jozsa, *Rapid solutions of problems by quantum computation*, Proceedings of the Royal Society of London A 439: 553. (1992)

[9] D. P. DiVincenzo, *The Physical Implementation of Quantum Computation*, `arXiv:quant-ph/0002077v3`

[10] C. H. Bennett et al., *Teleporting an Unknown Quantum State via Dual Classical and Einstein-Podolsky-Rosen Channels*, Phys. Rev. Lett. 70 1895-1899 (1993)

[11] M. Bourennane et al., *Decoherence-Free Quantum Information Processing with Four-Photon Entangled States*, `arXiv:quant-ph/0309041v2`

[12] C. H. Bennett et al., *Mixed State Entanglement and Quantum Error Correction*, `arXiv:quant-ph/9604024v2`

[13] J. A. Smolin, *A four-party unlockable bound-entangled state*, `arXiv:quant-ph/0001001v6`

[14] Y. Yu, *A quantum secret sharing scheme among three parties ultilizing four-qubit Smolin bound entangled state*, arXiv:quant-ph/0605225v2

[15] M. Murao, V. Vedral, *Remote information concentration using a bound entangled state*, arXiv:quant-ph/0008078v1

[16] M. Bourennane et al., *Experimental Detection of Multipartite Entanglement Using Witness Operators*, arXiv:quant-ph/0309043v2

[17] J. J. Sakurai, *Modern Quantum Mechanics*, Revised Edition, Addison-Wesley (1994), Boston MA, USA

[18] Wikipedia, *Inner product space*, http://en.wikipedia.org/w/index.php?title=Inner_product_space&oldid=129929783, Retrieved 22 May 2007

[19] Wikipedia, *Spectral Theorem*, http://en.wikipedia.org/w/index.php?title=Spectral_theorem&oldid=126975563, Retrieved 29 May 2007

[20] Wikipedia, *LOCC*, http://en.wikipedia.org/w/index.php?title=LOCC&oldid=114907245, Retrieved 2 June 2007

[21] M. Barbieri et al., *Complete and Deterministic discrimination of polarization Bell state assisted by momentum entanglement*, arXiv:quant-ph/0609080

[22] J. F. Clauser, M. A. Horne, *Experimental consequences of objective local theories*, Phys. Rev. D 10, 526 - 535 (1974)

[23] A. Peres, *Separability Criterion for Density Matrices*, arXiv:quant-ph/9604005

[24] M. Horodecki et al., *Separability of Mixed States: Necessary and Sufficient Conditions*, arXiv:quant-ph/9605038v2

[25] Wikipedia, *Entanglement Witness*, http://en.wikipedia.org/w/index.php?title=Entanglement_witness&oldid=90592618, Retrieved 31 May 2007

[26] Lewenstein et al., *Characterization of separable states and entanglement witnesses*, arXiv:quant-ph/0005112

[27] G. Toth, O. Gühne, *Entanglement Detection in the Stabilizer Formalism*, arXiv:quant-ph/0501020v2

[28] M. Horodecki et al., *Mixed-state entanglement and distillation: is there a "bound" entanglement in nature?*, arXiv:quant-ph/9801069v1

[29] A. Acín et al., *Classification of mixed three-qubit states*, arXiv:quant-ph/0103025

[30] P. Hyllus et al., *Generation and detection of bound entanglement*, arXiv:quant-ph/0405164

[31] P. Horodecki, *Separability criterion and inseparable mixed states with positive partial transposition*, arXiv:quant-ph/9703004v2

[32] J. Preskill, *Lecture Notes for Physics 229: Quantum Information and Computation*, California Institute of Technology (Sep 1998)

[33] E. Hecht, *Optics, 4th ed.*, Addison Wesley Longman, Inc. (2002), Reading MA, USA

[34] P. Kwiat et al., *Ultra-bright source of polarization-entangled photons*, arXiv:quant-ph/9810003v3

[35] R. Augusiak, P. Horodecki, *Bound entanglement maximally violating Bell inequalities: quantum entanglement is not equivalent to quantum security*, arXiv:quant-ph/0405187v2

[36] R. Augusiak, P. Horodecki, *Generalised Smolin states and their properties*, arXiv:quant-ph/0411142v1

[37] G. Wang, M. Ying, *Multipartite unlockable bound entanglement in the stabilizer formalism*, arXiv:quant-ph/0703033v3

ACKNOWLEDGEMENTS

Excellent!
- C. M. B.

Much appreciation go to my supervisor Docent Mohamed Bourennane for his advice, seemingly unlimited patience, and drive to find creative solutions to both practical and physical problems. Even though I was living in Uppsala while writing an "ex-jobb" in Stockholm, seeing him sparsely, he always came through 100% when it really mattered. The invitation to come and visit Uppsala still stands.

Mohamed also arranged the fantastic opportunity for me to go to the Max-Planck-Institut für Quantenoptik in Garching, Germany for a week in early 2005. The work there laid the foundation for the results on the unitary invariant states presented in this report. The warmly welcoming Max-Planck-Institut für Quantenoptik, and in particular, Geza Tóth, deserves all gratitude. Through the exhilarating 12-hour+ days, Geza served as my supervisor and provided invaluable insights into the theory of stabilizer witnesses, as well as the German cuisine. This excursion was in part funded by Dr. Herman Dahlins Scholarship from Värmlands nation, Uppsala, received in autumn 2004.

Sincere gratitude to my parents for everything, including hanging that nuclide chart over my crib. Great thanks to Alper, the Anderses, Björn, Fred, Ia, Johan, Mads, Nisse, Osfi and anyone who has ever gotten a head-ache from my rants beginning with "You see, you have four particles...". For the physics, the music and the good times.

MEMORABILIA

This is some crazy state!
Mohamed, on the Smolin state. Said more than once during our sessions held at KTH, Stockholm University and sometimes the cafés around Odenplan.

What is this? This is like, music, but it changes all the time!
Geza, probably uttering the most diplomatic thing anyone has ever said about Mattias IA Eklund's frenetic music and certainly about the piece "Print This!".

I think he is approaching the continuum limit...
The author, vacantly staring at the coffee list at KTH, where Björn Hessmo's tick-marks barely fit the page.